Identification of *C*-β-D-glucopyranosyl azole type inhibitors of glycogen phosphorylase that reduce glycogenolysis in hepatocytes: *in silico* design, synthesis, *in vitro* kinetics and *ex-vivo* studies

Daniel Barr,[a#] Eszter Szennyes,[b#] Éva Bokor,[b#] Ziad H. Al-Oanzi[c] Colin Moffatt,[d] Sándor Kun,[b] Tibor Docsa,[e] Ádám Sipos,[e] Matthew P. Davies,[a] Rachel Mathomes,[f] Timothy J. Snape,[f] Loranne Agius,*[c] László Somsák,*[b] Joseph M. Hayes*[f]

[a] *School of Physical Sciences & Computing, University of Central Lancashire, Preston PR1 2HE, United Kingdom*

[b] *Department of Organic Chemistry, University of Debrecen, POB 400, H-4002 Debrecen, Hungary*

[c] *Institute of Cellular Medicine, Newcastle University, Newcastle upon Tyne NE2 4HH, United Kingdom*

[d] *Health & Life Sciences, De Montfort University, Gateway House, Leicester. LE1 9BH, United Kingdom*

[e] *Department of Medical Chemistry, Medical and Health Science Centre, University of Debrecen, Egyetem tér 1, H-4032 Debrecen, Hungary*

[f] *School of Pharmacy & Biomedical Sciences, University of Central Lancashire, Preston PR1 2HE, United Kingdom*

[*] Corresponding authors
tel: +441912087033 (LA); email: loranne.agius@newcastle.ac.uk
tel: +3652512900 ext 22348 (LS); fax: +3652512744; e-mail: somsak.laszlo@science.unideb.hu
tel: +441772894334 (JMH); fax: +441772894981; email: jhayes@uclan.ac.uk
[#]Equal contribution

Contents

1. Computational Details

1.1 Protein Preparation

The initial setup of the GPb receptor for calculations was performed using Schrodinger's "Protein Preparation Wizard"[1] exploiting the solved co-crystallized complex with **5b** (PDB code: 5JTU)[2]. Water molecules common to 12 already solved GPb complexes (PDB codes: 5JTU, 5JTT, 3G2H, 3G2I, 3G2K, 3G2L, 1XL0, 1XL1, 5LRC, 5LRF, 5LRE and 5LRD) with β-D-glucopyranosyl analogues containing a 5-membered heterocyclic linker were retained using the Schrodinger cluster_waters.py script.[1] Bond orders were assigned and hydrogen atoms added, with protonation states for basic/acidic residues based on calculated residue *pKa* values from PROPKA[3] at normal pH (7.0). Subsequent optimization of hydroxyl groups, histidine protonation states and C/N atom "flips", and side-chain O/N atom flips of Asn and Gln residues was based on optimizing hydrogen bonding patterns. The phosphate group of pyridoxal-phosphate (PLP) was assigned its monoanionic form. Finally, an Impref minimization of the GPb complex was performed using the OPLS3 forcefield[4] to remove any steric clashes and bad contacts. At the end of the minimization, the RMSD of all heavy atoms was within 0.3 Å of the crystallographic positions.

1.2 Ligand Preparation

All ligands were prepared for calculations using LigPrep 3.9[1] with the protonation and tautomer states of the ligands generated at pH of 7.0 +/- 2.0. All predicted states were considered for the subsequent binding calculations. Additionally, to more accurately consider the relative stabilities of the tautomeric states of the unbound ligands, DFT calculations in the form of M06-2X[5] with the 6-31+G* basis set[6-7] gas phase optimizations followed by single point energy solution phase calculations were performed, with water solvation effects included using a

Solvation Model 8 (SM8) treatment.[8] Input conformations for the DFT calculations came from Monte Carlo Multiple Minima (MCMM) conformational searches (5000 steps, OPLS3 forcefield, GBSA water solvation model) using MacroModel v11.3[1], with the top 10 conformers considered. Finally, the potential of relevant heterocycles to be protonated (+1 charge) was also predicted using Epik and with Jaguar pKa calculations.[1]

1.3 Docking Details

Docking calculations were performed using Glide 7.2[1] and GOLD v5.4.1[9]. The protein structure used in each case was as per the Protein Preparation (4.1.1) with water molecules deleted, as their retention generally did not lead to improved results in initial tests.

Glide docking: The shape and properties of the GPb catalytic site were first mapped onto grids with dimensions of 27.0 × 27.0 × 27.0 Å centred on the native cocrystallized ligand. Given the effectiveness of docking geometry constraints in previous studies[10-12], both core constraints (0.75 Å) on the glucopyranose as well as positional constraints on its hydroxyl hydrogens (radius 0.75 Å) were applied to retain the moiety close to its known crystallographic position. Standard parameters were otherwise applied including default OPLS3 atomic charges and van der Waals scaling (0.8) for ligand nonpolar atoms to include modest 'induced fit' effects. Docking calculations were performed using both Glide-SP and -XP including post-docking minimization with strain correction. Up to 10 poses per input ligand structure were saved for each docking run in order to generate a large number of diverse poses.

GOLD docking: In the docking calculations with GOLD v5.4.1[9], all atoms and their associated residues within 10 Å of the ligand were used to define the active site. Information about the ligand hydrogen-bonding interactions and conformation was encoded into the corresponding genetics algorithms (GA) of GOLD with ChemPLP using the default GA parameters. Scaffold

constraints were placed on the glucose ring scaffold as well as the hydrogen atoms of its hydroxyl groups with a constraint weight of 5. Docking was set to generate 10 poses per ligand to achieve a large number of diverse poses.

1.4 MM-GBSA Calculations

Using Glide-SP and –XP, and GOLD-ChemPLP docking poses, MM-GBSA binding free energies were calculated using Prime 3.0 and the following equation:

$$\Delta G'_{bind} = \Delta E_{MM} + \Delta G_{solv} \qquad \text{Eq. (1)}$$

where ΔE_{MM} represents the molecular mechanics energy difference (internal, electrostatic and van der Waals) between the protein-ligand bound and unbound states calculated using the OPLS3 forcefield[4]. ΔG_{solv} is the corresponding solvation free energy change on binding calculated using a variable-dielectric generalized Born solvation model.

$\Delta G'_{bind}$ neglects the entropy (ΔS) contributions but for the best performing Prime models, ΔG_{bind} (Eq. 2) values were also calculated incorporating estimates for solute entropy changes. More specifically, the change in vibrational, rotational and translational (VRT) entropy of ligands on binding was calculated using the Rigid Rotor Harmonic Oscillator approximation (default settings) with MacroModel v11.3[1] and the OPLS3 forcefield[4].

$$\Delta G_{bind} = \Delta E_{MM} + \Delta G_{solv} - T\Delta S_{MM} \qquad \text{Eq. (2)}$$

The structures (bound and unbound) used in the $\Delta G'_{bind}$ and ΔG_{bind} calculations were taken from the Prime minimized complexes (protein constrained in minimization) and therefore included no strain/reorganization effects for the protein and ligand on binding. However, the effect of inclusion of ligand strain corrections to the binding free energies was also considered

and reported. As up to 10 docking poses per input ligand structures were used, the best $\Delta G'_{bind}$ and ΔG_{bind} values obtained for each inhibitor were taken as the predicted values for further analysis.

1.5 Physicochemical Property Predictions

Physicochemical properties of the ligands were calculated using QikProp 4.9[1] in normal mode. The input ligand structures used for these calculations were the most stable solution phase tautomers from the DFT calculations (4.1.2). Previous studies on β-D-glucopyranosyl heterocyclic derivatives revealing that the tautomeric state of the heterocycle has limited effect on the property predictions.[13-14] As more extended forms of ligands as input can lead to better agreement with experiment (QikProp User Manual), a MCMM conformational search was first performed for each inhibitor (5000 steps, OPLS3 forcefield, GBSA water solvation model) using MacroModel v11.3.[1] The most extended conformation based on calculated solvent accessible surface area (SASA)[1] was then used in the QikProp calculations.

1.6 Tables S1 and S2

Table S1. Full training set of ligands for model validation together with their inhibition constants (Ki's in µM) against rmGPb

		Aromatic R groups		
	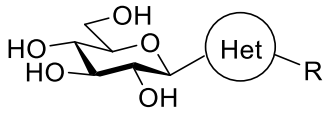	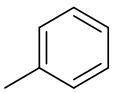	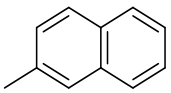	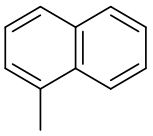
		a	**b**	**c**
1	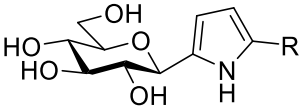	No inhibition at 625 µM. Ref[2]	No inhibition at 625 µM. Ref[2]	-
2	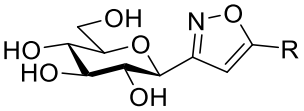	No inhibition at 625 µM. Ref[15]	No inhibition at 625 µM. Ref[15]	-
3	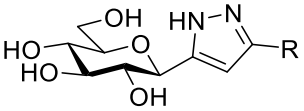	400 Ref[15]	-	-
4	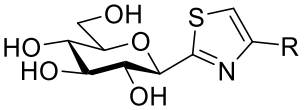	310 Ref[15]	158 Ref[15]	-
5	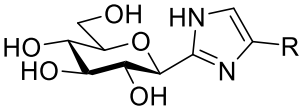	0.28 Ref[15]	0.031 Ref[15]	-
6	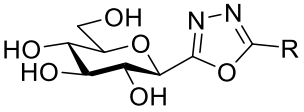	10% inhibition at 625 µM. Ref[16]	10% inhibition at 625 µM. Ref[16]	10% inhibition at 625 µM. Ref[16]
7	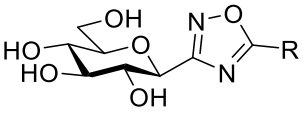	10% inhibition at 625 µM. Ref[16]	38 Ref[16]	No inhibition at 625 µM. Ref[16]
8	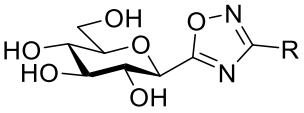	64 Ref[16]	11.6 Ref[16]	19 Ref[16]
9	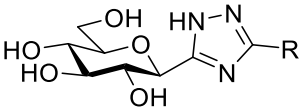	7 Ref[17]	0.41 Ref[17]	-[a]

14	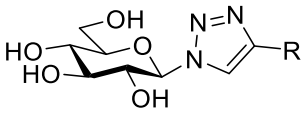	151 Ref[18]	16 Ref[18]	136 Ref[18]
15	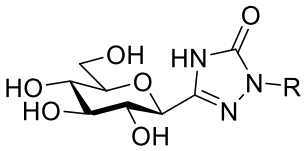	191 Ref[19]	80 Ref[19]	-
16	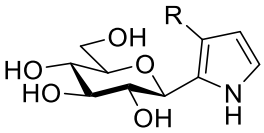	No inhibition at 625 µM. Ref[2]	No inhibition at 625 µM. Ref[2]	-

[a] Subsequently reported as 11.50 µM[13] and not part of training set.

Table S2. Predicted $\Delta G'_{bind}$ values (Eq.(1)) of target compounds using MM-GBSA *Model 2* as described in text.[a]

		Aromatic R groups		
	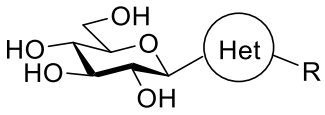	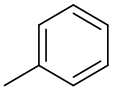	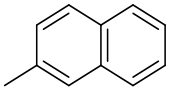	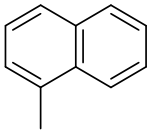
		a	**b**	**c**
3	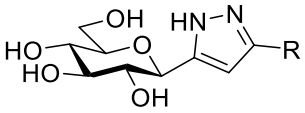	*-54.5*[b] *(-60.9)*[b]	-56.7[14] (-62.4[15])	-53.3[15] (-65.2[13])
5	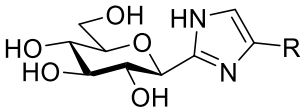	*-82.0*[b] *(-86.2)*[b]	*-87.9*[b] *(-92.4)*[b]	-85.2[1] (-93.8[1])
10	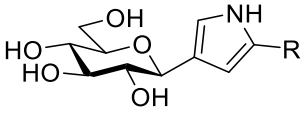	-66.2[8] (-70.0[11])	-69.5[5] (-73.8[5])	-64.6[9] (-72.6[7])
11	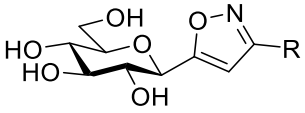	-66.3[7] (-71.0[9])	-68.6[6] (-73.8[5])	-64.3[10] (-71.2[8])
12	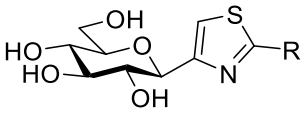	-58.3[12] (-63.7[14])	-58.7[11] (-66.8[12])	-57.0[13] (-70.6 [10])
13	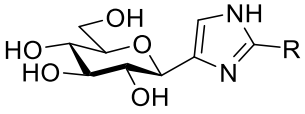	-72.4[4] (-78.9[4])	-78.5[3] (-86.7[3])	-79.5[2] (-88.9[2])

[a] Values *with* ligand strain correction with corresponding values *without* ligand strain correction given in parentheses. Predicted potency ranks for new ligands are given in square parentheses. [b] Training set ligand value shown for comparison.

2. Synthesis

2.1. General methods

Melting points were measured on a Kofler hot-stage and are uncorrected. Optical rotations were determined with a Perkin-Elmer 241 polarimeter at rt. NMR spectra were recorded with Bruker 360 (360/90 MHz for $^{1}H/^{13}C$) or Bruker 400 (400/100 MHz for $^{1}H/^{13}C$). Chemical shifts are referenced to the internal TMS (^{1}H), or to the residual solvent signals (^{13}C). The ^{13}C spectra for compounds **5c**, **12a-c**, **13a** and **15a-c** were recorded with the *J*-modulated spin-echo sequence to show all carbons (CH and CH_3 as positive while CH_2 and quaternary C as negative signals). Mass spectra were obtained by a Thermo Scientific LTQ XL or by a maXis II UHR ESI-TOF MS (Bruker) spectrometer. TLC was performed on DC-Alurolle Kieselgel 60 F_{254} (Merck), and the plates were visualised under UV light and by gentle heating (generally no spray reagent was used but, if more intense charring was necessary, the plate was sprayed with the following solution: abs. EtOH (95 mL), ccH_2SO_4 (5 mL) anisaldehyde (1 mL)). For column chromatography Kieselgel 60 (Merck, particle size 0.063-0.200 mm) was applied. $CHCl_3$ was distilled from P_4O_{10} and stored over 4 Å molecular sieves. MeOH was purified by distillation after refluxing for a couple of hours with magnesium turnings and iodine. Organic solutions were dried over anhydrous $MgSO_4$ and concentrated under diminished pressure at 40-60 ºC (water bath). Benzamidine hydrochloride (Sigma-Aldrich), thiobenzamide (Alfa Aesar), naphthalene-1-thiocarboxamide (Sigma-Aldrich) and 2-bromo-1-(1-naphthyl)ethanone (Sigma-Aldrich) were purchased from the indicated suppliers. Bromomethyl 2',3',4',6'-tetra-*O*-β-D-glucopyranosyl ketone[20] (**14**), *C*-(2,3,4,6-tetra-*O*-benzyl-β-D-glucopyranosyl)formamdine hydrochloride (**17**),[21-22] and naphthalene-2-carboxamidine hydrochloride[23] were synthesized according to literature procedures. Naphthalene-2-

thiocarboxamide[24] and naphthalene-1-carboxamidine hydrochloride[25] were obtained by adapting literature protocols.

2.2. General procedures

*2.2.1. General procedure I for the synthesis of 2-aryl-4-(2',3',4',6'-tetra-*O*-benzoyl-β-D-glucopyranosyl)-thiazoles (15)*

A solution of compound **14** (1 equiv.) and the corresponding aromatic thioamide (1 equiv.) in anhydrous DMF (3 mL / 100 mg substrate) was heated at 140 ^{o}C. After completion of the reaction monitored by TLC (96 : 4 toluene-EtOAc) the mixture was poured into water and extracted with ethyl acetate (5 x). The combined organic phase was dried over $MgSO_4$, filtered and evaporated. The residual crude product was purified by crystallization.

2.2.2. General procedure II for the synthesis of 2-aryl-4(5)-(3',4',6'-tri-O-benzoyl-β-D-glucopyranosyl)-imidazoles (16)

The corresponding arene carboxamidine hydrochloride (3 equiv.) and K_2CO_3 (4 equiv.) were stirred in a THF-H_2O solvent mixture (4 : 1, 5 mL / 100 mg substrate) at reflux temperature for 2 h. After cooling the reaction mixture at rt compound **14** (1 equiv.) was added and the stirring was continued at rt. When the TLC (3 : 2 hexane-EtOAc) showed total consumption of the starting material (1 d) the mixture was diluted with EtOAc and extracted with water. The organic phase was dried over $MgSO_4$, filtered, and evaporated under reduced pressure. The residue was purified by column chromatography.

2.2.3. General procedure III for removal of benzoyl protecting groups by the Zemplén protocol to get test compounds 12 and 13

To a solution or a suspension of an *O*-perbenzoylated compound in anhydrous MeOH-$CHCl_3$ solvent mixture (5 mL : 1mL/100 mg starting material, respectively) a catalytic amount of a NaOMe solution (~1 M in MeOH) was added. The reaction mixture was stirred at rt until the TLC (1 : 1 hexane-EtOAc and 3 : 1 $CHCl_3$-MeOH) showed complete transformation. The mixture was then neutralized with glacial acetic acid and the solvent was removed. The crude product was purified by column chromatography.

2.3. Syntheses and characterization of the compounds

4-(2',3',4',6'-Tetra-*O*-benzoyl-β-D-glucopyranosyl)-2-phenyl-thiazole (15a)

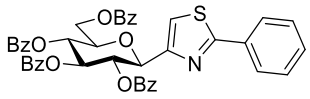

Prepared from compound **14** (0.20 g, 0.29 mmol) and thiobenzamide (39 mg, 0.29 mmol) according to General procedure I. Reaction time: 2 h. The crude product was purified by crystallization from EtOH to yield 0.16 g (74 %) white solid. Mp: 212-214 ºC; $[\alpha]_D$ = +14 (c 0.55, $CHCl_3$). ^{1}H NMR (400 MHz, $CDCl_3$) δ (ppm): 8.06-7.21 (26H, m, aromatics, thiazole CH), 6.09 (1H, pseudo t, *J* = 9.7, 9.6 Hz, H-3'), 5.88 (1H, pseudo t, *J* = 9.7, 9.6 Hz, H-2'), 5.85 (1H, pseudo t, *J* = 10.0, 9.7 Hz, H-4'), 5.12 (1H, d, *J* = 9.7 Hz, H-1'), 4.73 (1H, dd, *J* = 12.2, 3.0 Hz, H-6'a), 4.55 (1H, dd, *J* = 12.2, 4.8 Hz, H-6'b), 4.35 (1H, ddd, *J* = 10.0, 4.8, 3.0 Hz, H-5'); ^{13}C NMR (100 MHz, $CDCl_3$) δ (ppm): 168.4, 166.4, 166.0, 165.4, 165.3 (thiazole C-2, C=O), 153.0 (thiazole C-4), 133.5-126.6 (aromatics), 116.8 (thiazole CH), 76.7 (2), 74.5, 72.6, 69.9 (C-1' – C-5'), 63.4 (C-6'). ESI-MS positive mode (m/z): calcd for $C_{43}H_{34}NO_9S^+$ $[M+H]^+$: 740.2. Found: 740.5.

4-(2',3',4',6'-Tetra-*O*-benzoyl-β-D-glucopyranosyl)-2-(2-naphthyl)-thiazole (15b)

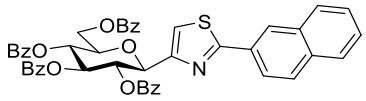

Prepared from compound **14** (0.25 g, 0.36 mmol) and naphthalene-2-thiocarboxamide (67 mg, 0.36 mmol) according to General procedure I. Reaction time: 2 h. Purified by crystallization from Et_2O to yield 207 mg (74 %) white solid. Mp: 232-233 ºC; $[\alpha]_D$ = +19 (c 0.22, $CHCl_3$); ^{1}H NMR (400 MHz, $CDCl_3$) δ (ppm): 8.08-7.27 (28H, m, aromatics, thiazole CH), 6.13 (1H, pseudo t, *J* = 9.1, 9.1 Hz, H-2' or H-3' or H-4'), 5.90-5.88 (2H, m, H-2' and/or H-3' and/or H-4'), 5.17 (1H, d, *J* = 9.1 Hz, H-1'), 4.75 (1H, dd, *J* = 12.3, < 1 Hz, H-6'a), 4.57 (1H, dd, *J* = 12.3, 2.1 Hz, H-6'b), 4.38 (1H, m, H-5'); ^{13}C NMR (100 MHz, $CDCl_3$) δ (ppm): 168.3, 166.2, 165.9, 165.2, 165.1 (thiazole C-2, C=O), 153.0 (thiazole C-4), 133.9-123.9 (aromatics), 116.7 (thiazole CH), 76.5 (2), 74.3, 72.4, 69.7 (C-1' – C-5'), 63.2 (C-6'). ESI-MS positive mode (m/z): calcd for $C_{47}H_{36}NO_9S^+$ $[M+H]^+$: 790.2; $C_{47}H_{35}NO_9SNa^+$ $[M+Na]^+$: 812.2. Found: $[M+H]^+$: 790.5; $[M+Na]^+$: 812.5.

4-(2',3',4',6'-Tetra-*O*-benzoyl-β-D-glucopyranosyl)-2-(1-naphthyl)-thiazole (15c)

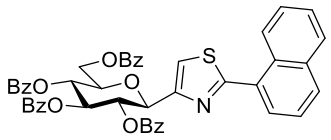

Prepared from compound **14** (0.50 g, 0.71 mmol) and naphthalene-1-thiocarboxamide (133 mg, 0.71 mmol) according to General procedure I. Reaction time: 2 h. The crude product was purified by crystallization from EtOH to yield 0.48 g (85 %) white solid. Mp: 186-187 ºC; $[\alpha]_D$ = +46 (c 0.26, $CHCl_3$). ^{1}H NMR (360 MHz, $CDCl_3$) δ (ppm): 8.52-7.22 (28H, m, aromatics, H-5), 6.12 (1H, pseudo t, *J* = 9.5 9.4 Hz, H-2' or H-3' or H-4'), 6.05 (1H, pseudo t, *J* = 9.5 9.4 Hz, H-2' or H-3' or H-4'), 5.90 (1H, pseudo t, *J* = 9.4 9.4 Hz, H-2' or H-3' or H-4'), 5.24 (1H, d, *J* = 9.5 Hz, H-1'), 4.72 (1H, dd, *J* = 12.2, 2.1 Hz, H-6'a), 4.57 (1H, dd, *J* = 12.2, 4.6 Hz, H-

6'b), 4.40-4.37 (1H, m, H-5'); ^{13}C NMR (90 MHz, $CDCl_3$) δ (ppm): 167.8, 166.3, 166.0, 165.4, 165.2 (C-2, C=O), 152.6 (C-4), 133.5-124.9 (aromatics), 118.6 (C-5), 76.9, 76.8, 74.7, 72.7, 69.9 (C-1' – C-5'), 63.5 (C-6'). ESI-MS positive mode (m/z): calcd for $C_{47}H_{36}NO_9S^+$ $[M+H]^+$: 790.2105; $C_{47}H_{35}NNaO_9S^+$ $[M+Na]^+$: 812.1925. Found: $[M+H]^+$: 790.2100; $[M+Na]^+$: 812.1919.

4-(β-D-Glucopyranosyl)-2-phenyl-thiazole (12a)

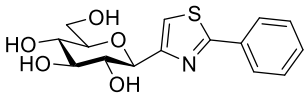

Prepared from compound **15a** (0.40 g, 0.54 mmol) according to General procedure III. Reaction time: 18 h. Purified by column chromatography (9 : 1 $CHCl_3$-MeOH) to yield 0.15 g (87 %) white amorphous solid. R_f = 0.54 (4 : 1 $CHCl_3$-MeOH); $[\alpha]_D$ = +17 (c 0.32, MeOH). ^{1}H NMR (400 MHz, CD_3OD) δ (ppm): 7.96-7.94 (2H, m, aromatics), 7.57 (1H, s, thiazole CH), 7.49-7.45 (2H, m, aromatics), 4.42 (1H, d, *J* = 9.6 Hz, H-1'), 3.89 (1H, dd, *J* = 12.1, 2.0 Hz, H-6'a), 3.74 (1H, pseudo t, *J* = 9.4, 9.2 Hz, H-2' or H-3' or H-4'), 3.72 (1H, dd, *J* = 12.1, 5.4 Hz, H-6'b), 3.56-3.44 (3H, m, H-2' and/or H-3' and/or H-4', H-5'); ^{13}C NMR (100 MHz, CD_3OD) δ (ppm): 170.0, 156.4 (thiazole C-2, C-4), 134.7, 131.4, 130.2, 127.7, 127.5 (aromatics), 119.0 (thiazole C-5), 82.2, 79.6, 79.0, 74.9 (C-1' – C-5'), 71.4 (C-6'). ESI-MS positive mode (m/z): calcd for $C_{15}H_{17}NO_5SNa^+$ $[M+Na]^+$: 346.0720; $C_{30}H_{34}N_2O_{10}S_2Na^+$ $[2M+Na]^+$: 669.1547. Found: $[M+Na]^+$: 346.0723; $[2M+Na]^+$: 669.1553.

4-(β-D-Glucopyranosyl)-2-(2-naphthyl)-thiazole (12b)

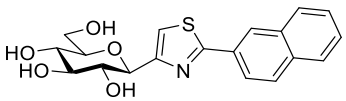

Prepared from compound **15b** (0.20 g, 0.25 mmol) according to General procedure III. Reaction time: 5 d. Purified by column chromatography (9 : 1 $CHCl_3$-MeOH) to yield 93 mg

(98 %) colourless syrup. R_f = 0.47 (7 : 3 $CHCl_3$-MeOH); $[\alpha]_D$ = –45 (c 0.25, MeOH). ^{1}H NMR (360 MHz, CD_3OD) δ (ppm): 8.43 (1H, s, aromatic), 8.04-7.86 (4H, m, aromatics), 7.59 (1H, s, thiazole CH), 7.54-7.51 (2H, m, aromatics), 4.45 (1H, d, *J* = 9.5 Hz, H-1'), 3.91 (1H, dd, *J* = 12.3, 1.8 Hz, H-6'a), 3.82-3.49 (5H, m, H-2', H-3', H-4', H-5', H-6'b). ^{13}C NMR (90 MHz, CD_3OD) δ (ppm): 170.0, 156.6 (thiazole C-2, C-4), 135.6, 134.7, 132.0, 130.0, 129.7, 128.9, 128.4, 128.1, 127.1, 124.9 (aromatics), 119.2 (thiazole CH), 82.3, 79.7, 79.1, 74.9, 71.5 (C-1' – C-5'), 63.0 (C-6'). ESI-MS positive mode (m/z): calcd for $C_{19}H_{19}NO_5SNa^+$ $[M+Na]^+$: 396.0876; $C_{38}H_{38}N_2O_{10}S_2Na^+$ $[2M+Na]^+$: 769.1860. Found: $[M+Na]^+$: 396.0883; $[2M+Na]^+$: 769.1872.

4-(β-D-Glucopyranosyl)-2-(1-naphthyl)-thiazole (12c)

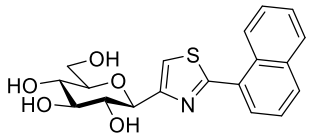

Prepared from compound **15c** (0.30 g, 0.38 mmol) according to General procedure III. Reaction time: 1 d. Purified by column chromatography (9 : 1 $CHCl_3$-MeOH) to yield 131 mg (92 %) colourless syrup. R_f = 0.65 (7 : 3 $CHCl_3$-MeOH); $[\alpha]_D$ = +37 (c 0.23, MeOH). ^{1}H NMR (360 MHz, CD_3OD) δ (ppm): 8.55-7.49 (7H, m, aromatics), 7.70 (1H, s, H-5), 4.51 (1H, d, *J* = 9.5 Hz, H-1'), 3.89 (1H, dd, *J* = 12.0, 1.9 Hz, H-6'a), 3.81 (1H, pseudo t, *J* = 9.5, 9.1 Hz, H-2'), 3.74 (1H, dd, *J* = 12.0, 4.9 Hz, H-6'b), 3.59 (1H, pseudo t, *J* = 9.3, 9.1 Hz, H-3' or H-4'), 3.55 (1H, pseudo t, *J* = 9.3, 9.1 Hz, H-3' or, H-4'), 3.50-3.47 (1H, m, H-5'). ^{13}C NMR (90 MHz, CD_3OD) δ (ppm): 169.1, 156.0 (C-2, C-4), 135.3, 131.9, 131.7 (2), 129.6, 129.4, 128.3, 127.6, 126.6, 126.1 (aromatics), 120.1 (C-5), 82.1, 79.6, 79.0, 75.0, 71.2 (C-1' – C-5'), 62.8 (C-6'). ESI-MS positive mode (m/z): calcd for $C_{19}H_{20}NO_5S^+$ $[M+H]^+$: 374.1057; $C_{19}H_{19}NNaO_5S^+$ $[M+Na]^+$: 396.0876. Found: $[M+H]^+$: 374.1054; $[M+Na]^+$: 396.0880.

4(5)-(3',4',6'-Tri-*O*-benzoyl-β-D-glucopyranosyl)-2-phenyl-imidazole (16a)

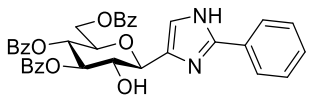

Prepared from compound **14** (0.50 g, 0.71 mmol) and benzamidine hydrochloride (0.22 g, 1.43 mmol) according to General procedure II. Purified by column chromatography (3 : 2 hexane-EtOAc) to yield 0.20 g (45 %) pale yellow syrup. R_f = 0.32 (1 : 1 hexane-EtOAc); $[\alpha]_D$ = +1 (c 0.36, $CHCl_3$). ^{1}H NMR (360 MHz, $CDCl_3$) δ (ppm): 10.20 (1H, broad s, NH), 8.04-7.26 (20H, m, aromatics), 7.05 (1H, s, imidazole CH), 5.80 (1H, pseudo t, *J* = 9.7, 9.4 Hz, H-3'), 5.65 (1H, pseudo t, *J* = 9.8, 9.7 Hz, H-4'), 4.64 (1H, d, *J* = 9.5 Hz, H-1'), 4.62 (1H, dd, *J* = 12.2, 2.9 Hz, H-6'a), 4.49 (1H, dd, *J* = 12.2, 5.0 Hz, H-6'b), 4.22-4.14 (2H, m, H-2', H-5'); ^{13}C NMR (90 MHz, $CDCl_3$) δ (ppm): 166.7, 166.5, 165.8 (C=O), 146.4 (imidazole C-2), 139.0 (imidazole C-4), 133.4-125.4 (aromatics), 116.4 (imidazole CH), 76.7, 76.4, 76.2, 73.4, 70.2 (C-1' – C-5'), 63.9 (C-6'). ESI-MS positive mode (m/z): calcd for $C_{36}H_{31}N_2O_8^+$ $[M+H]^+$: 619.2. Found: 619.5.

4(5)-(3',4',6'-Tri-*O*-benzoyl-β-D-glucopyranosyl)-2-(2-naphthyl)-imidazole (16b)

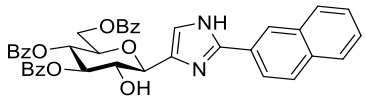

Prepared from compound **14** (0.20 g, 0.29 mmol) and naphthalene-2-carboxamidine hydrochloride (0.12 g, 0.57 mmol) according to General procedure II. Purified by column chromatography (3 : 2 hexane-EtOAc) to yield 0.09 g (49 %) pale yellow syrup. R_f = 0.51 (1 : 1 hexane-EtOAc); $[\alpha]_D$ = +10 (c 0.39, $CHCl_3$); ^{1}H NMR (360 MHz, $CDCl_3$) δ (ppm): 10.77 (1H, broad s, NH), 8.12-7.24 (22H, m, aromatics), 7.07 (1H, s, imidazole CH), 5.82 (1H, pseudo t, *J* = 9.7, 9.4 Hz, H-3'), 5.65 (1H, pseudo t, *J* = 9.8, 9.7 Hz, H-4'), 4.64 (1H, d, *J* = 9.5 Hz, H-1'), 4.58 (1H, dd, *J* = 12.2, 3.0 Hz, H-6'a), 4.45 (1H, dd, *J* = 12.2, 5.0 Hz, H-6'b), 4.23 (1H, pseudo t, *J* = 9.5, 9.4 Hz, H-2'), 4.14 (1H, ddd, *J* = 9.8, 5.0, 3.0 Hz, H-5'). ^{13}C NMR (90

MHz, $CDCl_3$) δ (ppm): 166.8, 166.5, 165.8 (C=O), 146.5 (imidazole C-2), 139.1 (imidazole C-4), 133.4-123.1 (aromatics), 116.6 (imidazole CH), 76.8, 76.2, 76.0, 73.3, 70.2 (C-1' – C-5'), 63.9 (C-6'). ESI-MS positive mode (m/z): calcd for $C_{40}H_{33}N_2O_8^+$ $[M+H]^+$: 669.2. Found: 669.5.

4(5)-(3',4',6'-Tri-*O*-benzoyl-β-D-glucopyranosyl)-2-(1-naphthyl)-imidazole (16c)

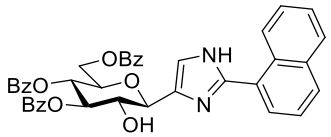

Prepared from compound **14** (0.5 g, 0.71 mmol) and naphthalene-1-carboxamidine hydrochloride (0.3 g, 1.45 mmol) according to General procedure II. Purified by column chromatography (3 : 2 hexane-EtOAc) to yield 0.19 g (39 %) pale yellow syrup. R_f = 0.34 (1 : 1 hexane-EtOAc); $[\alpha]_D$ = +17 (c 0.22, $CHCl_3$); ^{1}H NMR (360 MHz, $CDCl_3$) δ (ppm): 10.86 (1H, broad s, NH), 8.43-8.41, 7.95-7.21 (22H, m, aromatics), 6.99 (1H, s, imidazole CH), 5.70, 5.59 (2 × 1H, 2 pseudo t, *J* = 9.4, 9.4 Hz in each, H-3', H-4'), 4.54-4.48 (2H, m, H-1', H-6'a), 4.40 (1H, dd, *J* = 12.1, 5.1 Hz, H-6'b), 4.13 (1H, pseudo t, *J* = 9.4, 9.4 Hz, H-2'), 4.01-3.98 (1H, m, H-5'); ^{13}C NMR (90 MHz, $CDCl_3$) δ (ppm): 166.7, 166.4, 165.6 (C=O), 145.8 (imidazole C-2), 139.4 (imidazole C-4), 133.8-125.0 (aromatics), 115.3 (imidazole CH), 76.5, 76.0, 75.8, 73.0, 69.8 (C-1' – C-5'), 63.7 (C-6'). ESI-MS positive mode (m/z): calcd for $C_{40}H_{33}N_2O_8^+$ $[M+H]^+$: 669.2. Found: 669.5.

4(5)-(β-D-Glucopyranosyl)-2-phenyl-imidazole (13a)

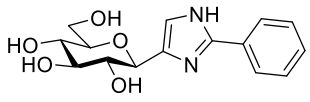

Prepared from compound **16a** (0.30 g, 0.48 mmol) according to General procedure III. Reaction time: 3 h. Purified by column chromatography (7 : 1 $CHCl_3$-MeOH) to yield 0.12 g (82 %) colourless syrup. R_f = 0.44 (7 : 3 $CHCl_3$-MeOH); $[\alpha]_D$ = –16 (c 0.28, MeOH). ^{1}H NMR (400

MHz, CD_3OD) δ (ppm): 7.88-7.85 (2H, m, aromatics), 7.46-7.35 (3H, m, aromatics), 7.18 (1H, s, imidazole CH), 4.32 (1H, d, *J* = 9.6 Hz, H-1'), 3.89 (1H, dd, *J* = 11.9, 1.8 Hz, H-6'a), 3.71 (1H, dd, *J* = 11.9, 5.1 Hz, H-6'b), 3.63 (1H, pseudo t, *J* = 9.6, 9.3 Hz, H-2' or H-3' or H-4'), 3.52-3.44 (3H, m, H-2' and/or H-3' and/or H-4', H-5'); ^{13}C NMR (100 MHz, CD_3OD) δ (ppm): 148.1, 137.3 (imidazole C-2, C-4), 131.2, 129.9, 126.5 (aromatics), 121.4 (imidazole CH), 81.8, 79.7, 76.5, 74.6, 71.5 (C-1' – C-5'), 62.9 (C-6'). ESI-MS positive mode (m/z): calcd for $C_{15}H_{19}N_2O_5^+$ $[M+H]^+$: 307.1288; $C_{30}H_{36}N_4O_{10}Na^+$ $[2M+Na]^+$: 635.2324. Found: $[M+H]^+$: 307.1290; $[2M+Na]^+$: 635.2327.

4(5)-(β-D-Glucopyranosyl)-2-(2-naphthyl)-imidazole (13b)

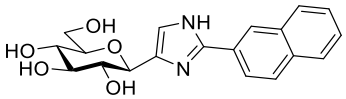

Prepared from compound **16b** (0.20 g, 0.30 mmol) according to General procedure III. Reaction time: 3 h. Purified by column chromatography (7 : 1 $CHCl_3$-MeOH) to yield 0.09 g (85 %) white amorphous solid. R_f = 0.50 (7 : 3 $CHCl_3$-MeOH); $[\alpha]_D$ = –25 (c 0.33, MeOH). ^1H NMR (400 MHz, CD_3OD) δ (ppm): 8.35 (1H, s, aromatic), 8.03-7.87 (4H, m, aromatics), 7.55-7.49 (2H, m, aromatics), 7.23 (1H, s, imidazole CH), 4.35 (1H, d, *J* = 9.4 Hz, H-1'), 3.90 (1H, dd, *J* = 11.7, 1.6 Hz, H-6'a), 3.73 (1H, dd, *J* = 11.7, 4.7 Hz, H-6'b), 3.65 (1H, pseudo t, *J* = 9.4, 9.4 Hz, H-2' or H-3' or H-4'), 3.53-3.46 (3H, m, H-2' and/or H-3' and/or H-4', H-5'); ^{13}C NMR (90 MHz, CD_3OD) δ (ppm): 148.1, 137.5 (imidazole C-2, C-4), 134.8, 129.7, 129.3, 128.8, 128.6, 127.8, 127.7, 125.5, 124.2 (aromatics), 121.7 (imidazole CH), 81.9, 79.7, 76.6, 74.7, 71.5 (C-1' – C-5'), 63.0 (C-6'). ESI-MS positive mode (m/z): calcd for $C_{19}H_{21}N_2O_5^+$ $[M+H]^+$: 357.1445; $C_{38}H_{40}N_4O_{10}Na^+$ $[2M+Na]^+$: 735.2637. Found: $[M+H]^+$: 357.1445; $[2M+Na]^+$: 735.2639.

4(5)-(β-D-Glucopyranosyl)-2-(1-naphthyl)-imidazole (13c)

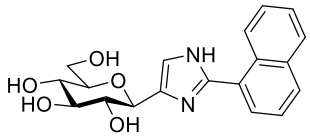

Prepared from compound **16c** (0.16 g, 0.24 mmol) according to General procedure III. Reaction time: 3 h. Purified by column chromatography (85 : 15 $CHCl_3$-MeOH) to yield 69 mg (81 %) colourless syrup. R_f = 0.50 (7 : 3 $CHCl_3$-MeOH); $[\alpha]_D$ = –38 (c 0.22, MeOH). ^{1}H NMR (360 MHz, CD_3OD) δ (ppm): 8.38-8.34 (1H, m, aromatic), 7.97-7.90 (2H, m, aromatics), 7.69-7.66 (1H, m, aromatic), 7.56-7.51 (3H, m, aromatics), 7.31 (1H, s, imidazole CH), 4.39 (1H, d, *J* = 9.6 Hz, H-1'), 3.89 (1H, dd, *J* = 12.6, 1.8 Hz, H-6'a), 3.73-3.67 (2H, m, H-2' or H-3' or H-4', H-6'b), 3.56-3.46 (3H, m, H-2' and/or H-3' and/or H-4', H-5'); ^{13}C NMR (90 MHz, CD_3OD) δ (ppm): 147.4, 137.3 (imidazole C-2, C-4), 135.3, 132.5, 130.7, 129.4, 128.5, 127.8, 127.3, 126.8, 126.2 (aromatics), 120.9 (imidazole CH), 81.8, 79.7, 76.6, 74.8, 71.5 (C-1' – C-5'), 62.9 (C-6'). ESI-MS positive mode (m/z): calcd for $C_{19}H_{21}N_2O_5^+$ $[M+H]^+$: 357.1445; $C_{38}H_{40}N_4O_{10}Na^+$ $[2M+Na]^+$: 735.2637. Found: $[M+H]^+$: 357.1449; $[2M+Na]^+$: 735.2643.

2-(2',3',4',6'-Tetra-*O*-benzyl-β-D-glucopyranosyl)-4(5)-(1-naphthyl)-imidazole (18)

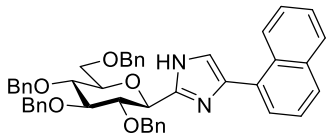

C-(2,3,4,6-Tetra-*O*-benzyl-β-D-glucopyranosyl)formamidine hydrochloride (**17**, 1.00 g, 1.66 mmol) and K_2CO_3 (0.46 g, 3.32 mmol, 2 equiv.) were suspended in a THF-H_2O solvent mixture (40 mL and 10 mL, respectively) and stirred at rt. After 15 min., 2-bromo-1-(1-naphthyl)ethanone (0.41 g, 1.66 mmol, 1 equiv.) was added to the reaction mixture and the stirring was continued at rt until the TLC (9 : 1 $CHCl_3$-MeOH and 1 : 1 hexane-EtOAc) showed disappearance of the starting material (2 d). The mixture was then diluted with EtOAc (200 mL) and extracted with water (2 × 100 mL). The organic layer was dried over $MgSO_4$, filtered

and the solvent was removed under reduced pressure. The resulting crude product was purified by column chromatography (1 : 1 hexane-EtOAc). Yield: 536 mg (45 %), yellow syrup. R_f = 0.63 (2 : 3 hexane-EtOAc); $[\alpha]_D$ = –52 (c 0.29, $CHCl_3$). ^{1}H NMR (360 MHz, $CDCl_3$) δ (ppm): 8.25-6.96 (28H, m, aromatics, imidazole CH), 4.92, 4.81 (2 x 1H, 2d, *J* = 11.0 Hz, $PhCH_2$), 4.72, 4.37 (2 x 1H, 2d, *J* = 10.8 Hz, $PhCH_2$), 4.66 (1H, d, *J* = 9.5 Hz, H-1'), 4.54, 4.29 (2 x 1H, 2d, *J* = 10.4 Hz, $PhCH_2$), 4.26, 4.21 (2 x 1H, 2d, *J* = 12.2 Hz, $PhCH_2$), 4.04 (1H, pseudo t, *J* = 9.3, 9.1 Hz, H-2'), 3.81 (1H, pseudo t, *J* = 9.3, 9.3 Hz, H-3'), 3.63 (1H, pseudo t, *J* = 9.3, 9.1 Hz, H-4'), 3.46-3.36 (3H, m, H-5', H-6'a, H-6'b); ^{13}C NMR (90 MHz, $CDCl_3$) δ (ppm): 145.2, 139.7 (imidazole C-2, C-4), 138.6, 138.2, 138.0, 137.4, 133.8, 131.3, 128.3-127.5 (aromatics), 116.1 (imidazole C-5), 86.5, 82.2, 78.8, 77.9, 75.5 (C-1' – C-5'), 75.1, 75.0, 74.8, 73.1 (4 × $PhCH_2$), 68.6 (C-6'). ESI-MS positive mode (m/z): calcd for $C_{47}H_{45}N_2O_5^+$ $[M+H]^+$: 717.3. Found: 717.7.

2-(β-D-Glucopyranosyl)-4(5)-(1-naphthyl)-imidazole (5c)

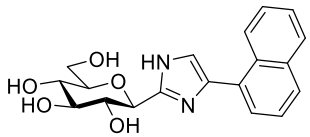

Compound **18** (0.44 g, 0.61 mmol) was dissolved in anhydrous CH_2Cl_2 (20 mL), EtSH (1.82 mL, 24.55 mmol, 40 equiv.) and $BF_3 \cdot Et_2O$ (1.52 mL, 12.28 mmol, 20 equiv.) were added. The reaction mixture was stirred at rt until the TLC (1 : 1 hexane-EtOAc and 3 : 1 $CHCl_3$-MeOH) indicated total consumption of **7** (3d). The mixture was then diluted with EtOAc (20 mL) and extracted with water (3 × 5 mL). The combined aqueous phases were concentrated under diminished pressure. The residue was purified by column chromatography (19 : 1 → 9 : 1 $CHCl_3$-MeOH) to give 130 mg (59 %) pale yellow syrup. R_f = (4 : 1 $CHCl_3$-MeOH); $[\alpha]_D$ = –11 (c 0.19, MeOH). ^{1}H NMR (360 MHz, CD_3OD) δ (ppm): 7.91-7.46 (7H, m, aromatics), 7.26 (1H, s, imidazole CH), 4.44 (1H, d, *J* = 9.7 Hz, H-1'), 3.90 (1H, dd, *J* = 12.2, 1.9 Hz, H-6'a),

3.75 (1H, dd, *J* = 12.2, 4.6 Hz, H-6'a) 3.73, 3.54 (2 × 1H, 2 pt, H-2' and/or H-3' and/or H-4'), 3.52-3.47 (2H, m, H-2' or H-3' or H-4', H-5'); ^{13}C NMR (90 MHz, CD_3OD) δ (ppm): 147.6, 136.8 (imidazole C-2, C-4), 135.3, 132.7, 131.3, 129.4, 129.2, 128.0, 127.3, 126.9, 126.6, 126.3 (aromatics), 120.7 (imidazole CH), 82.0, 79.3, 76.8, 74.6, 71.2 (C-1' – C-5'), 62.7 (C-6'). ESI-MS positive mode (m/z): calcd for $C_{19}H_{21}N_2O_5^+$ $[M+H]^+$: 357.1445; $C_{38}H_{40}N_4O_{10}Na^+$ $[2M+Na]^+$: 735.2637. Found: $[M+H]^+$: 357.1446; $[2M+Na]^+$: 735.2641.

2.4. ^{1}H and ^{13}C NMR spectra for the new compounds

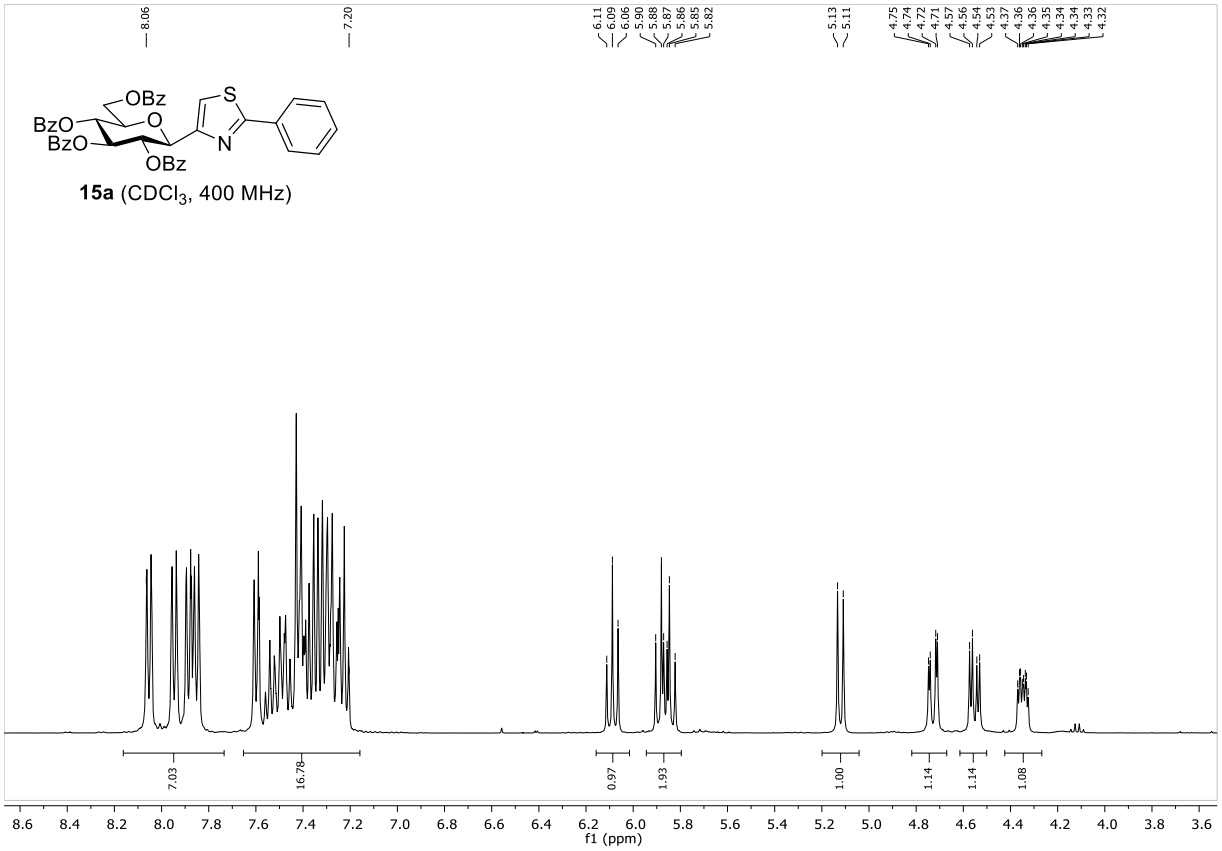

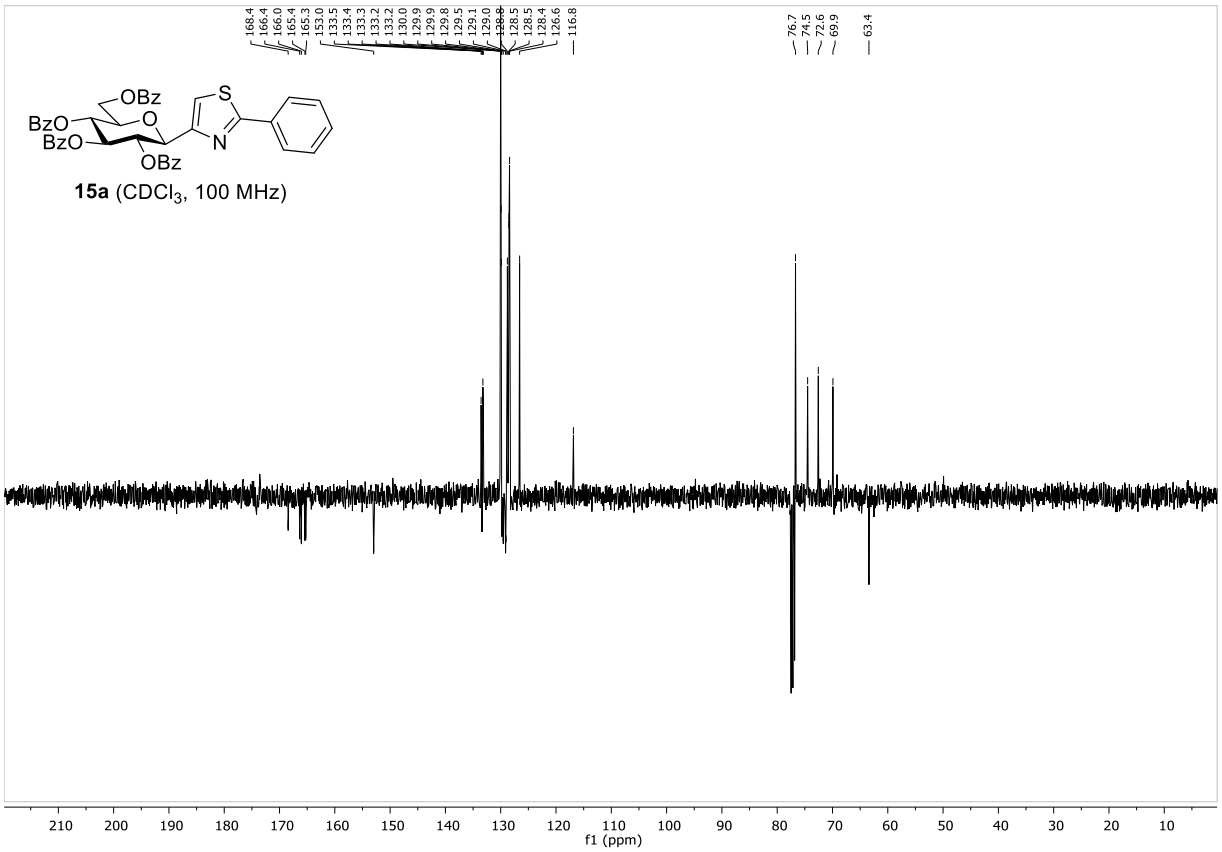

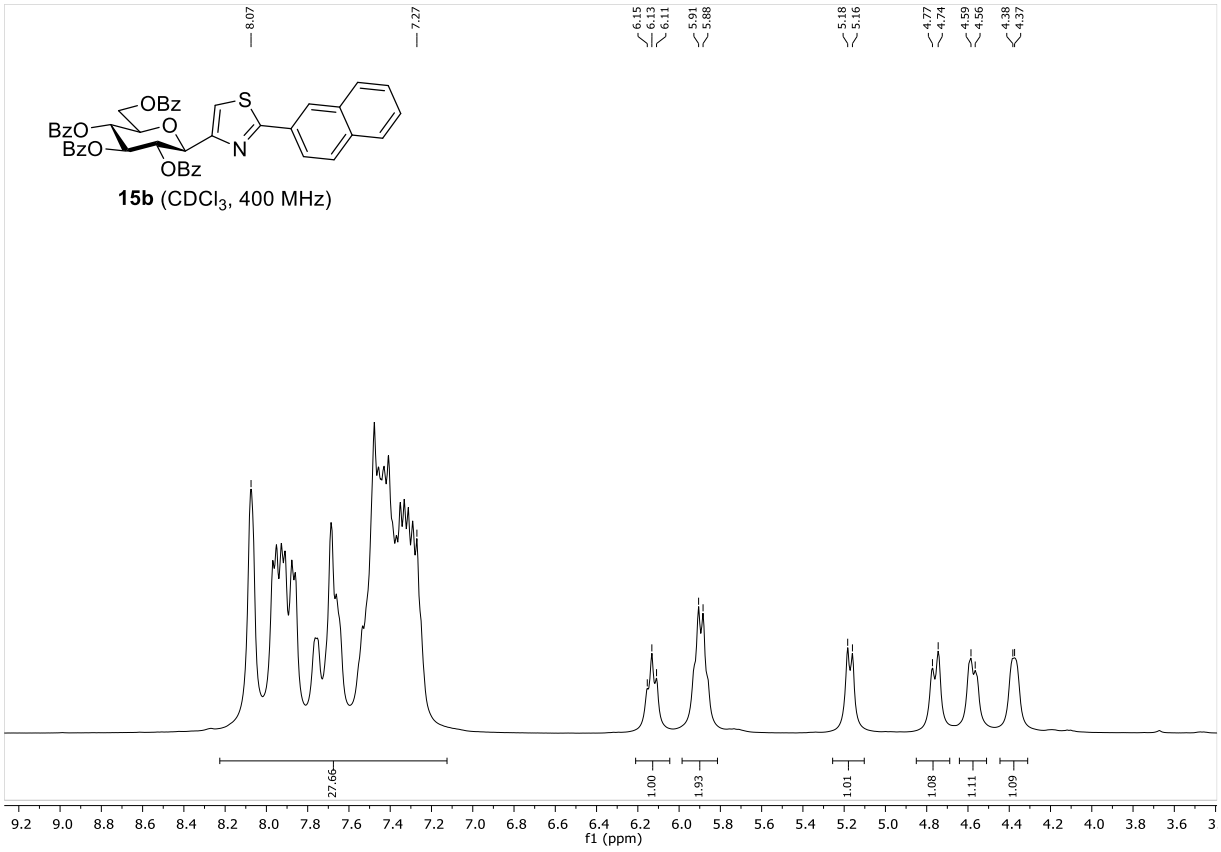

15b ($CDCl_3$, 400 MHz)

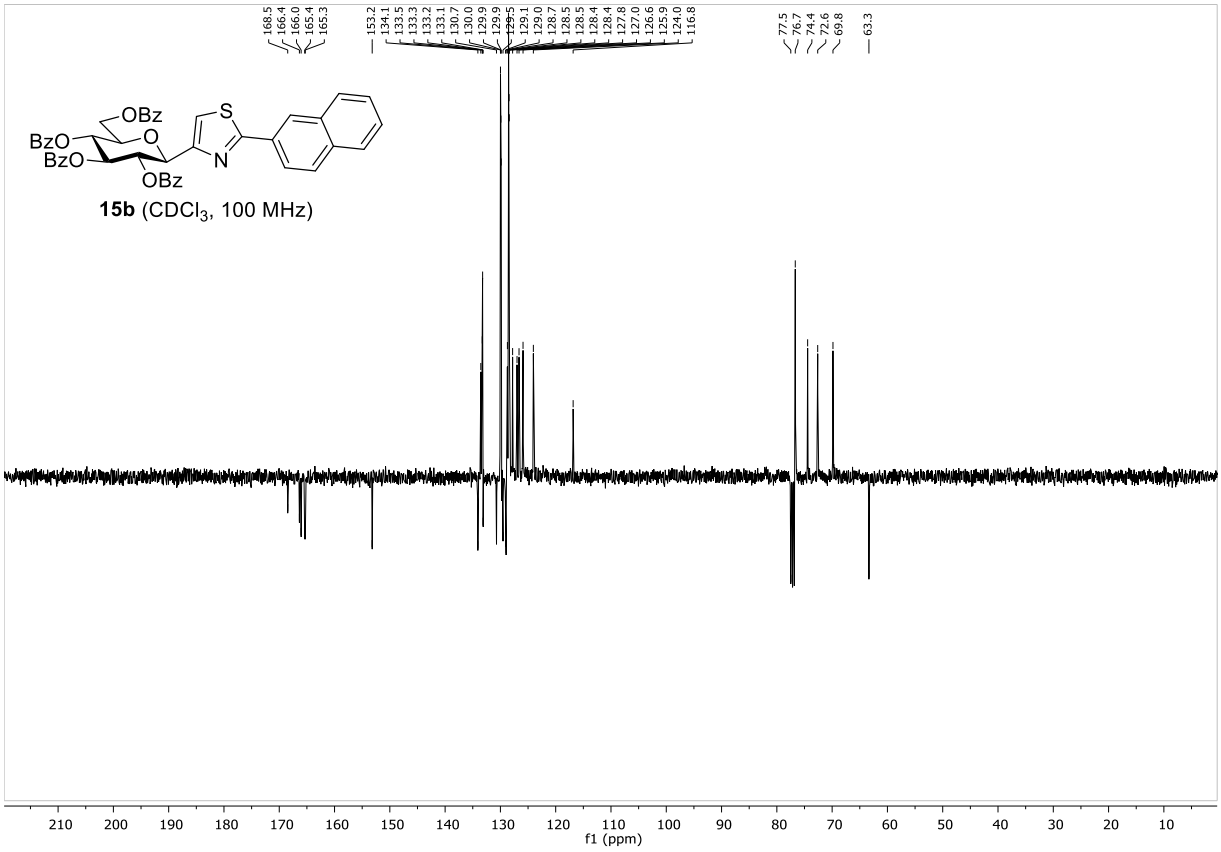

15b ($CDCl_3$, 100 MHz)

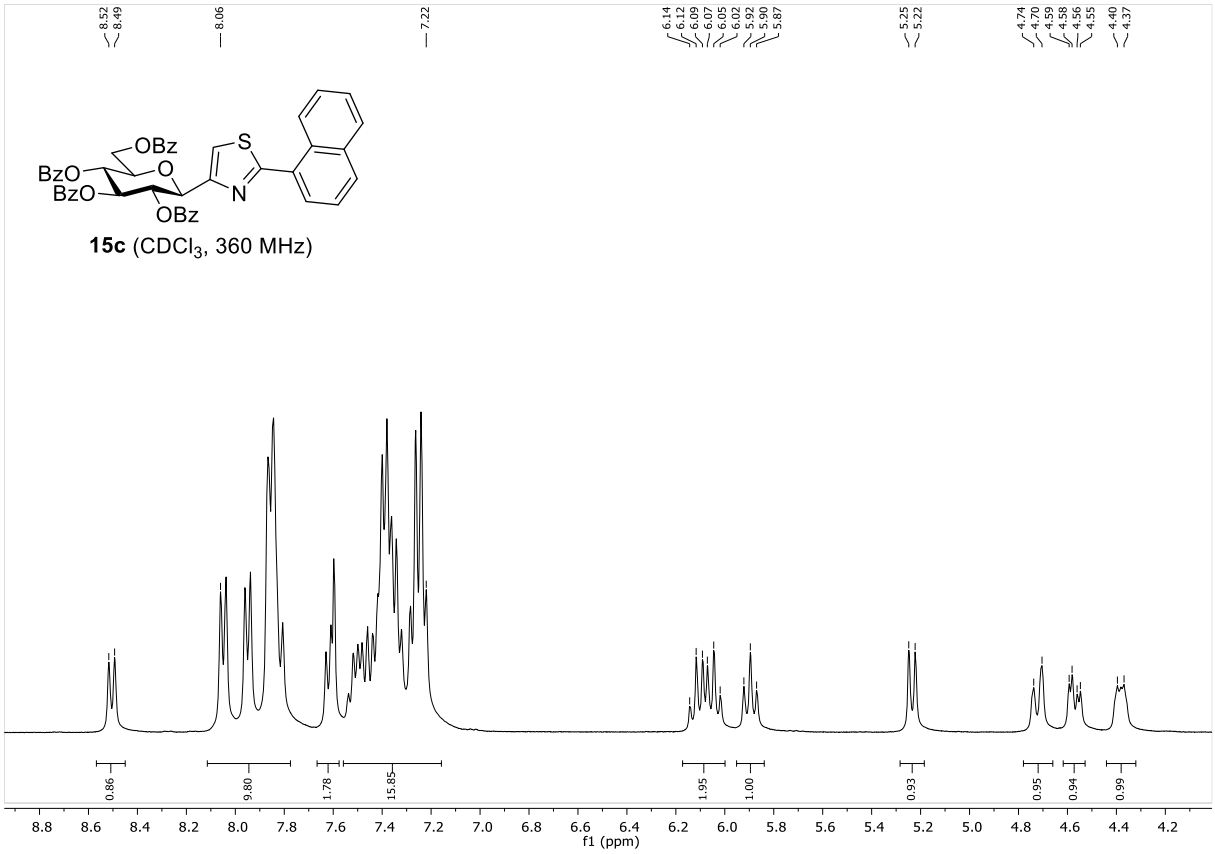
8.52
8.49
8.06
7.22
6.14
6.12
6.09
6.07
6.05
6.02
5.92
5.90
5.87
5.25
5.22
4.74
4.70
4.59
4.58
4.56
4.55
4.40
4.37
OBz
BzO
BzO
OBz
O
S
N
15c (CDCl3, 360 MHz)
0.86
9.80
1.78
15.85
1.95
1.00
0.93
0.95
0.94
0.99
f1 (ppm)

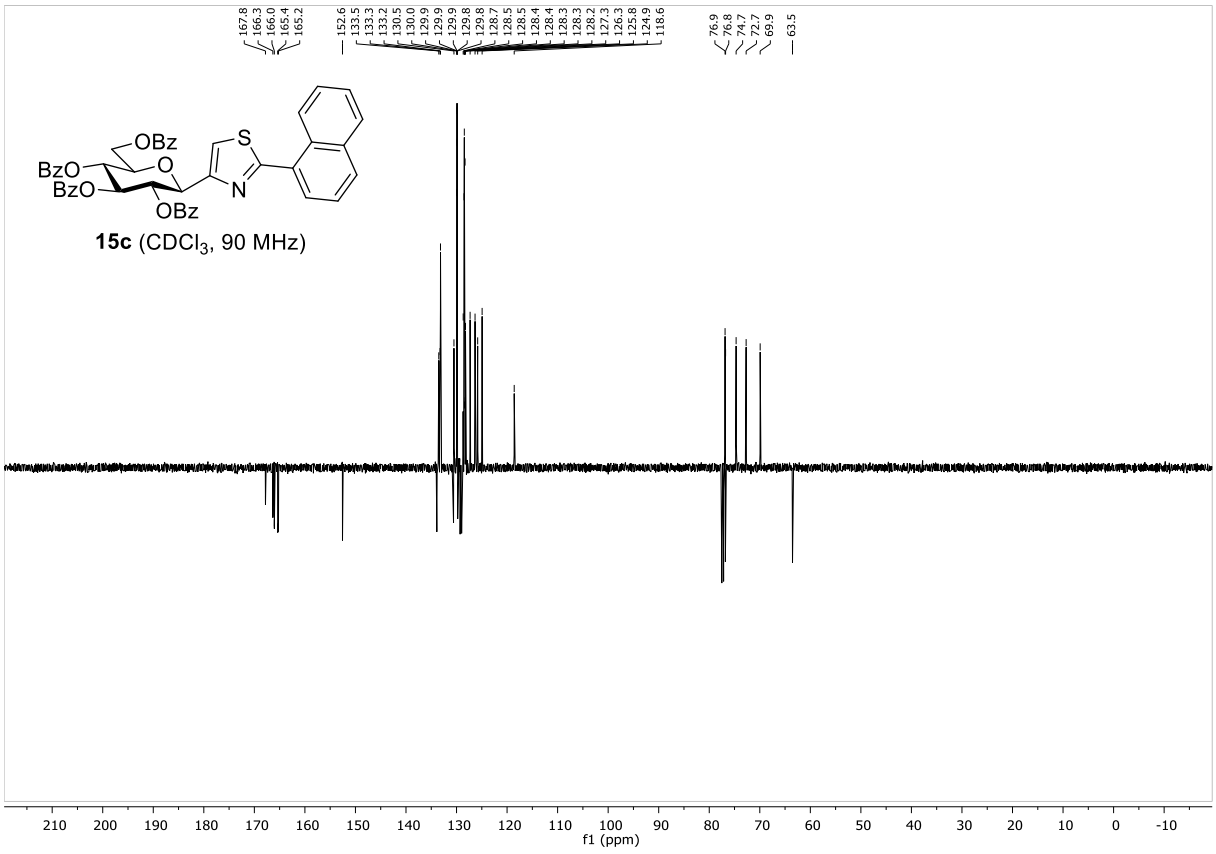
167.8
166.3
166.0
165.4
165.2
152.6
133.5
133.3
133.2
130.5
130.0
129.9
129.9
129.9
129.8
129.8
128.7
128.5
128.5
128.4
128.4
128.3
128.3
128.2
127.3
126.3
125.8
124.9
118.6
76.9
76.8
74.7
72.7
69.9
63.5
OBz
BzO
BzO
OBz
O
S
N
15c (CDCl3, 90 MHz)
f1 (ppm)

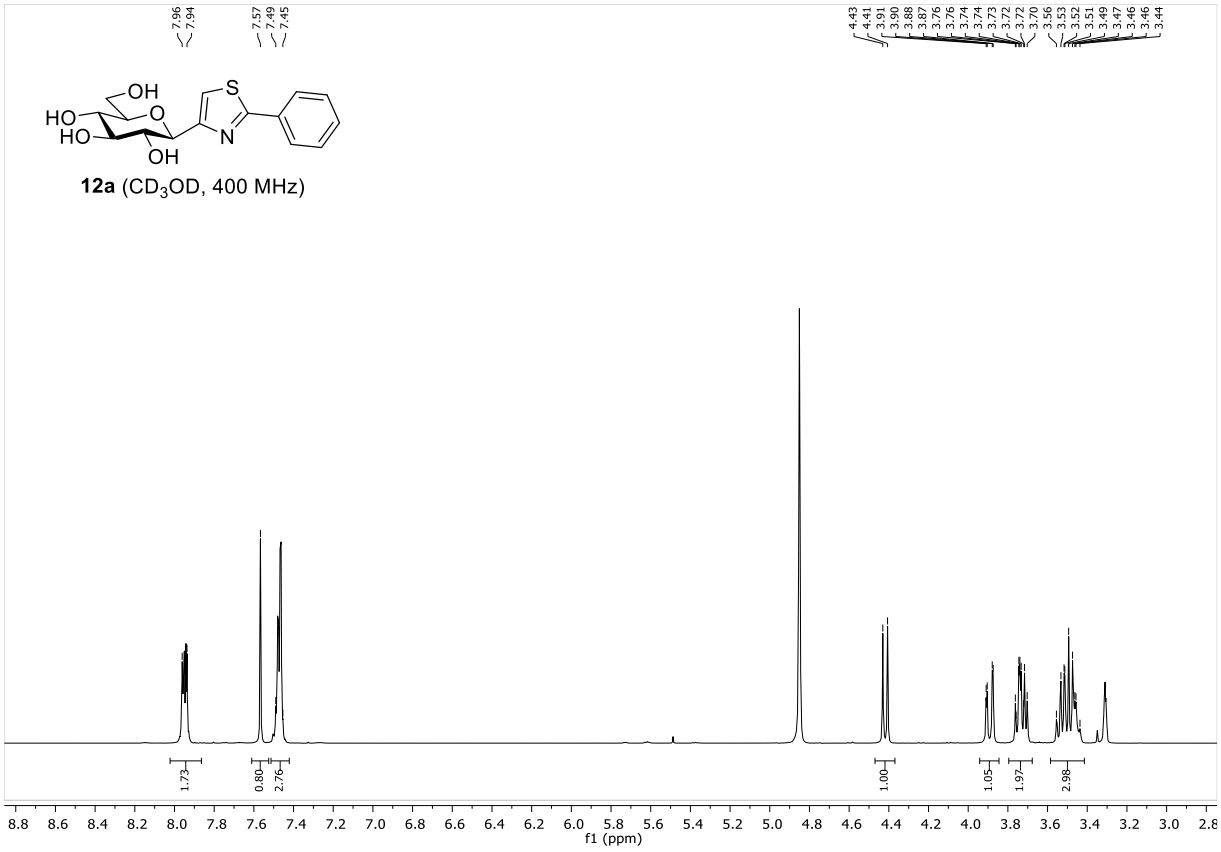

12a (CD_3OD, 400 MHz)

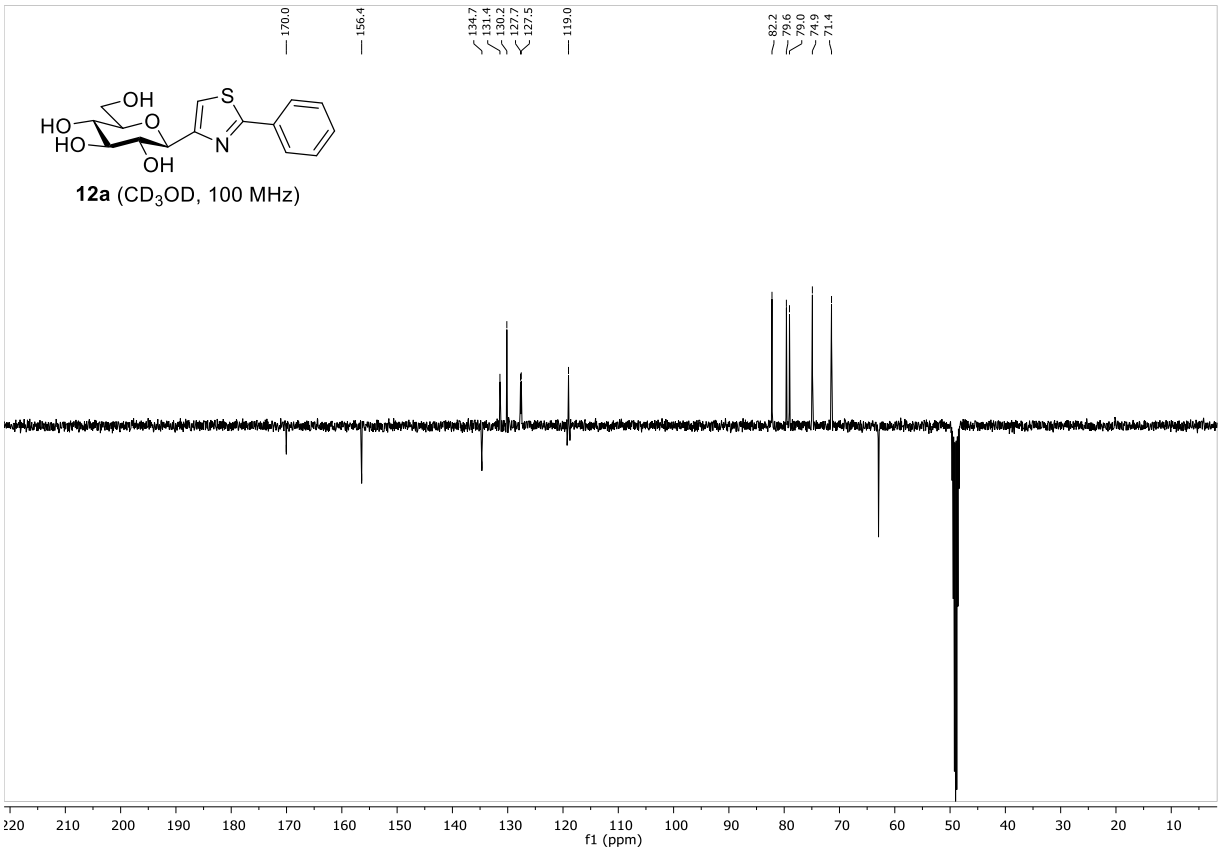

12a (CD_3OD, 100 MHz)

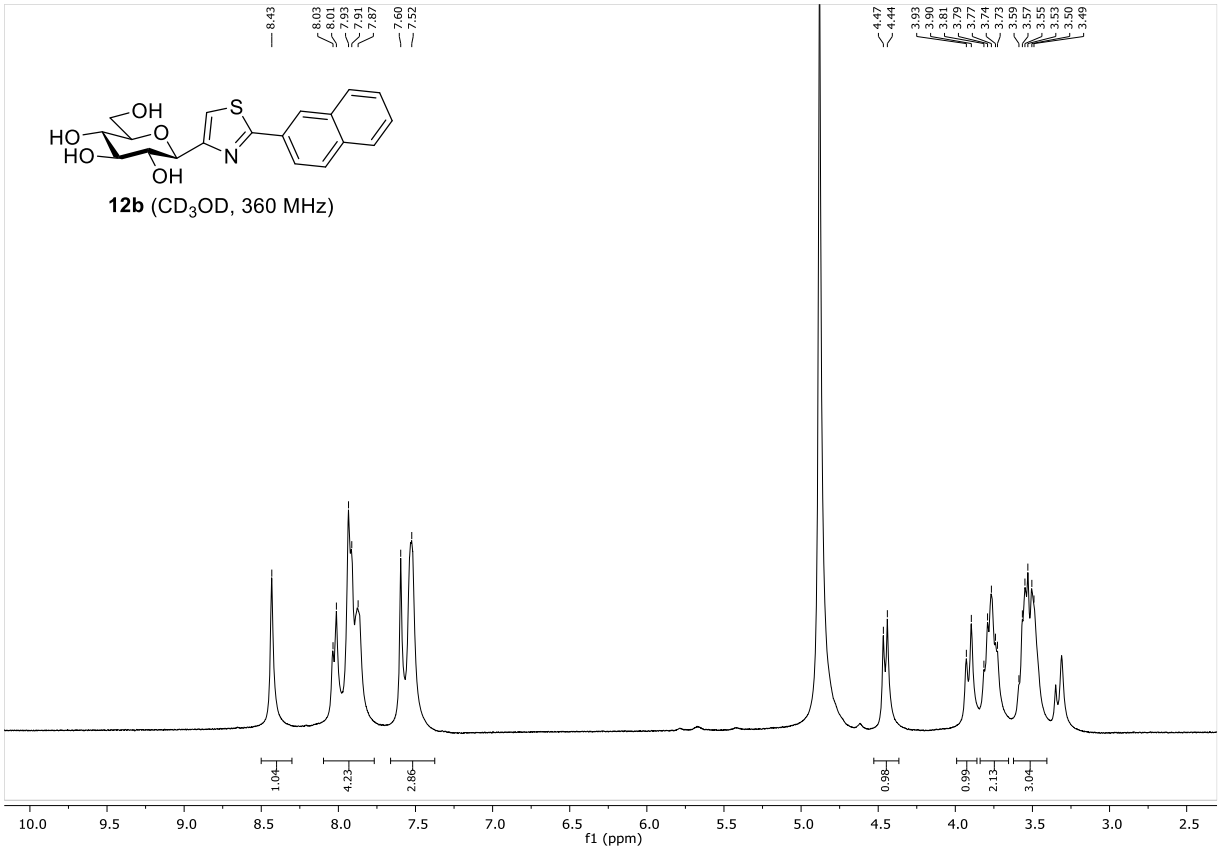

12b (CD_3OD, 360 MHz)

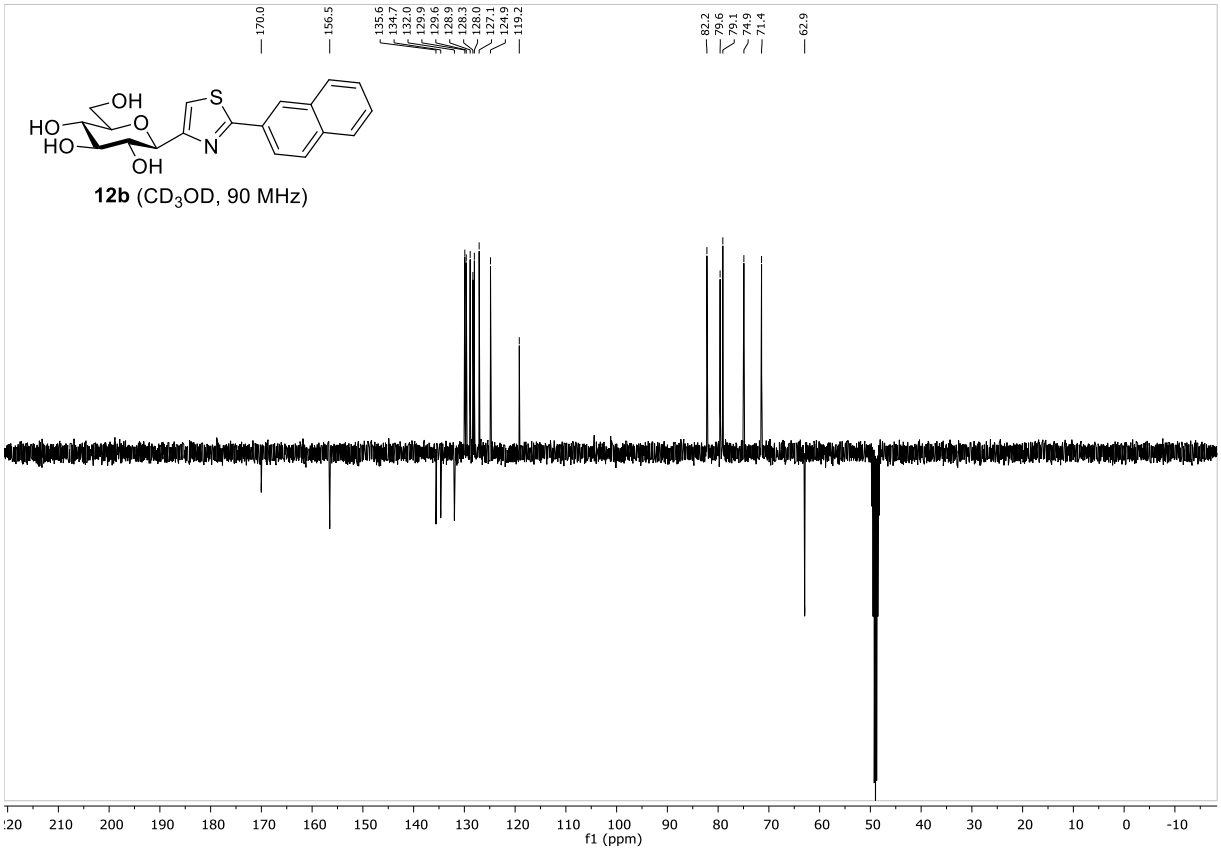

12b (CD_3OD, 90 MHz)

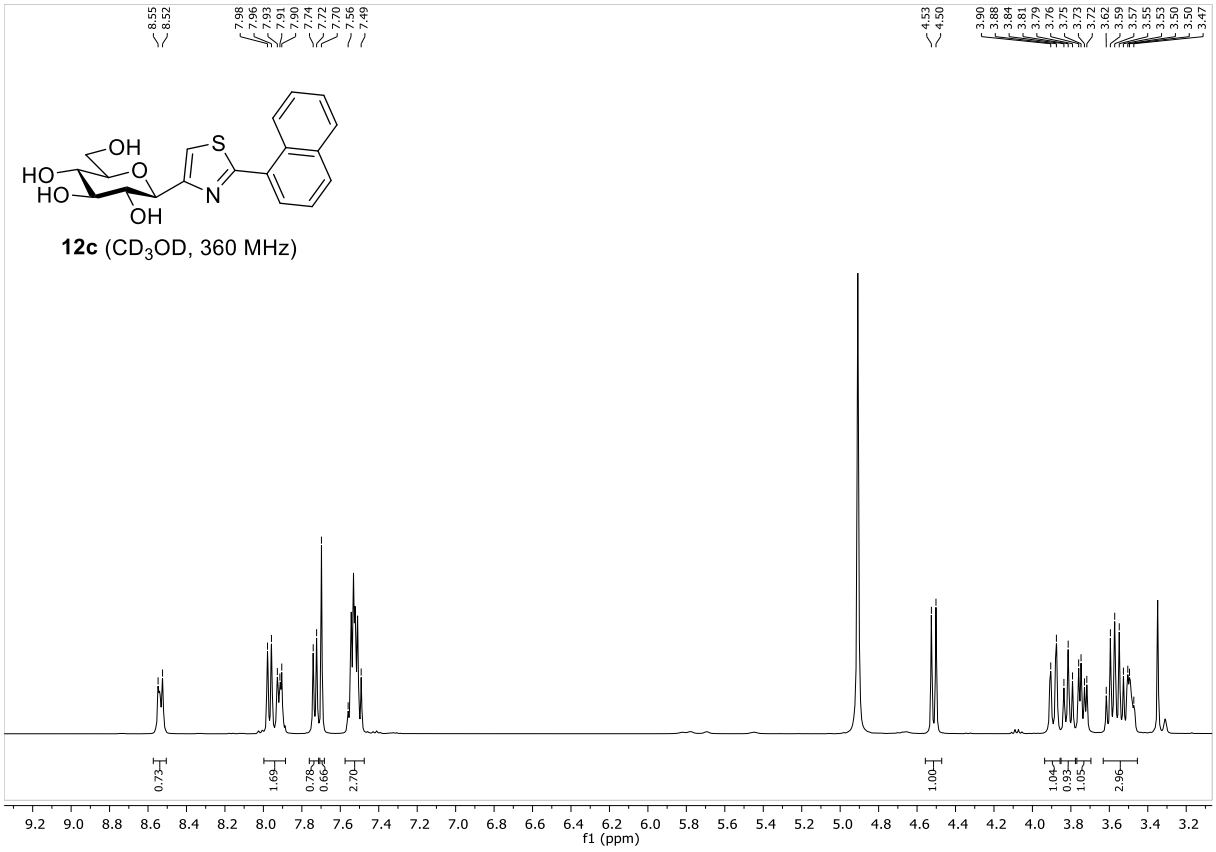

12c (CD_3OD, 360 MHz)

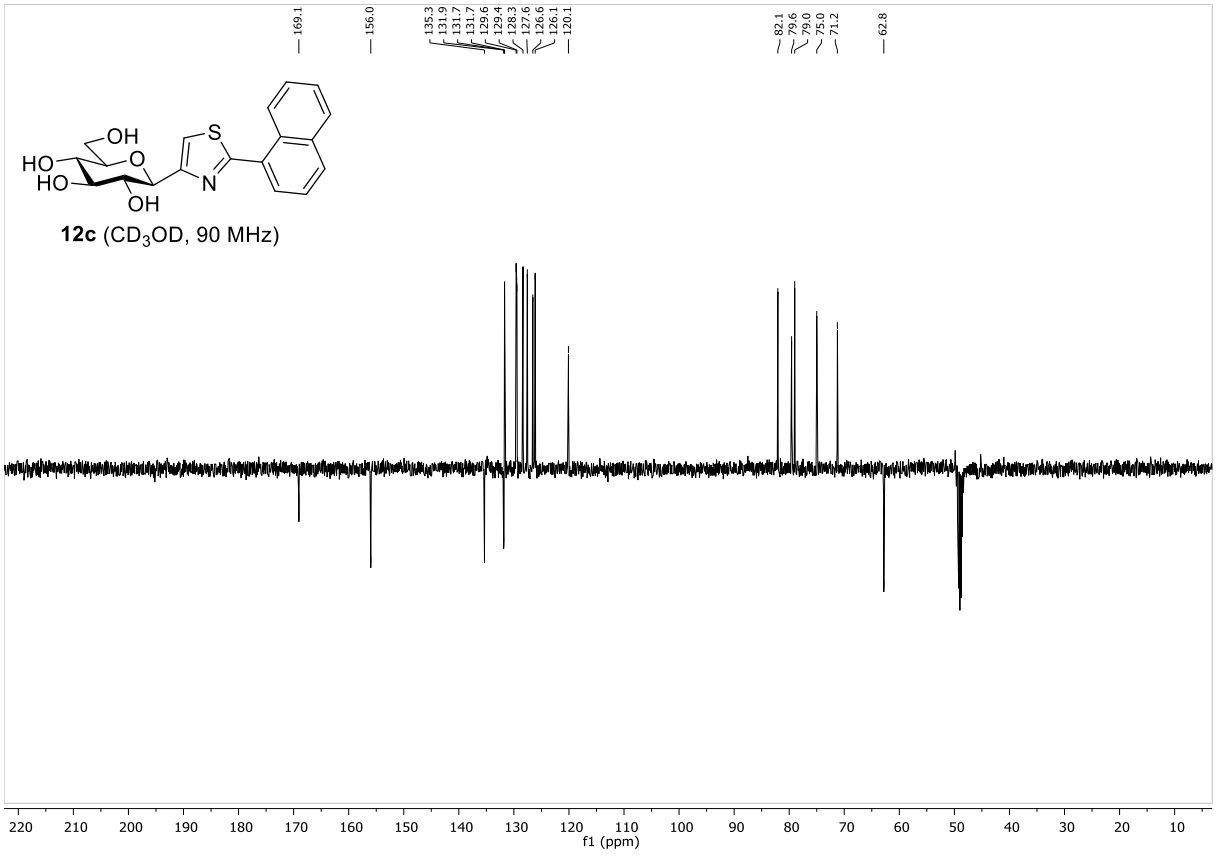

12c (CD_3OD, 90 MHz)

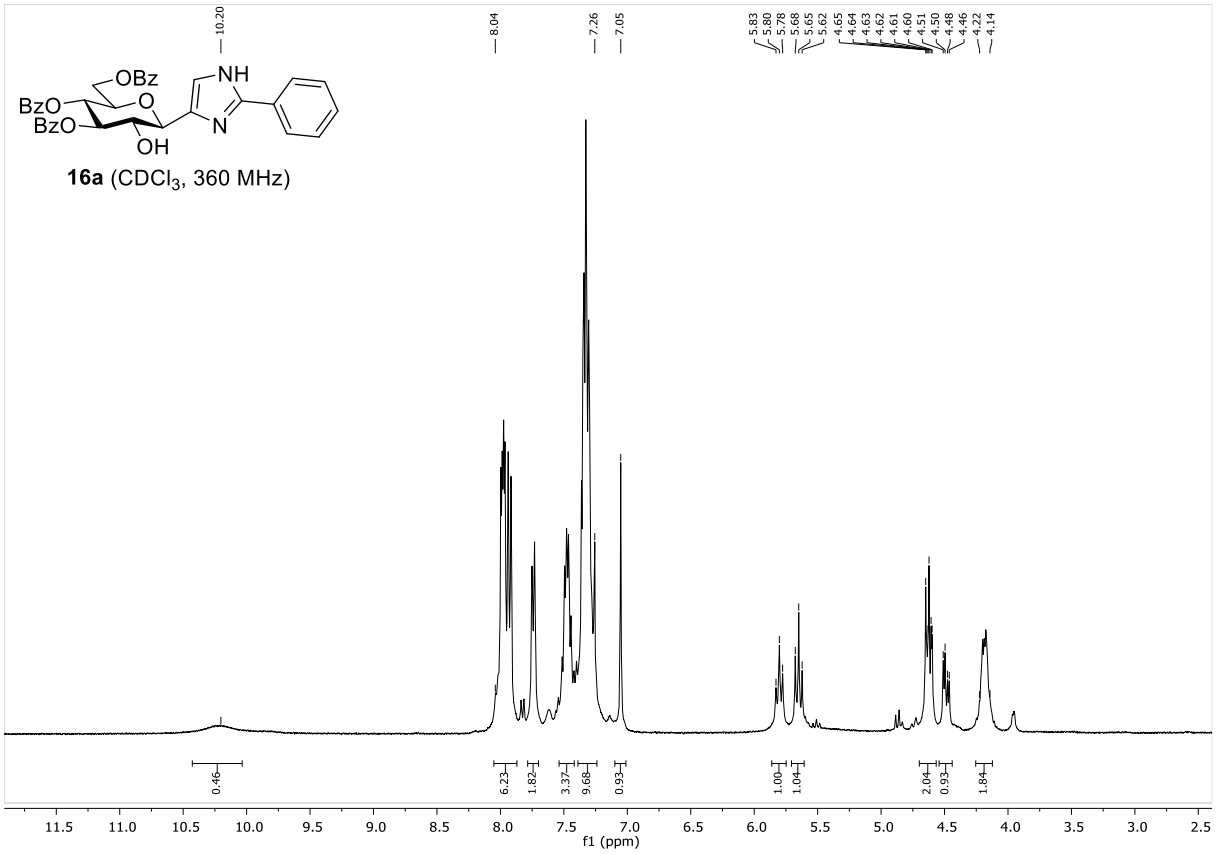
10.20
8.04
7.26
7.05
5.83
5.80
5.78
5.68
5.65
5.62
4.65
4.64
4.63
4.62
4.61
4.60
4.51
4.50
4.48
4.46
4.22
4.14
OBz
NH
BzO
O
BzO
N
OH
16a (CDCl3, 360 MHz)
0.46
6.23
1.82
3.37
9.68
0.93
1.00
1.04
2.04
0.93
1.84
f1 (ppm)

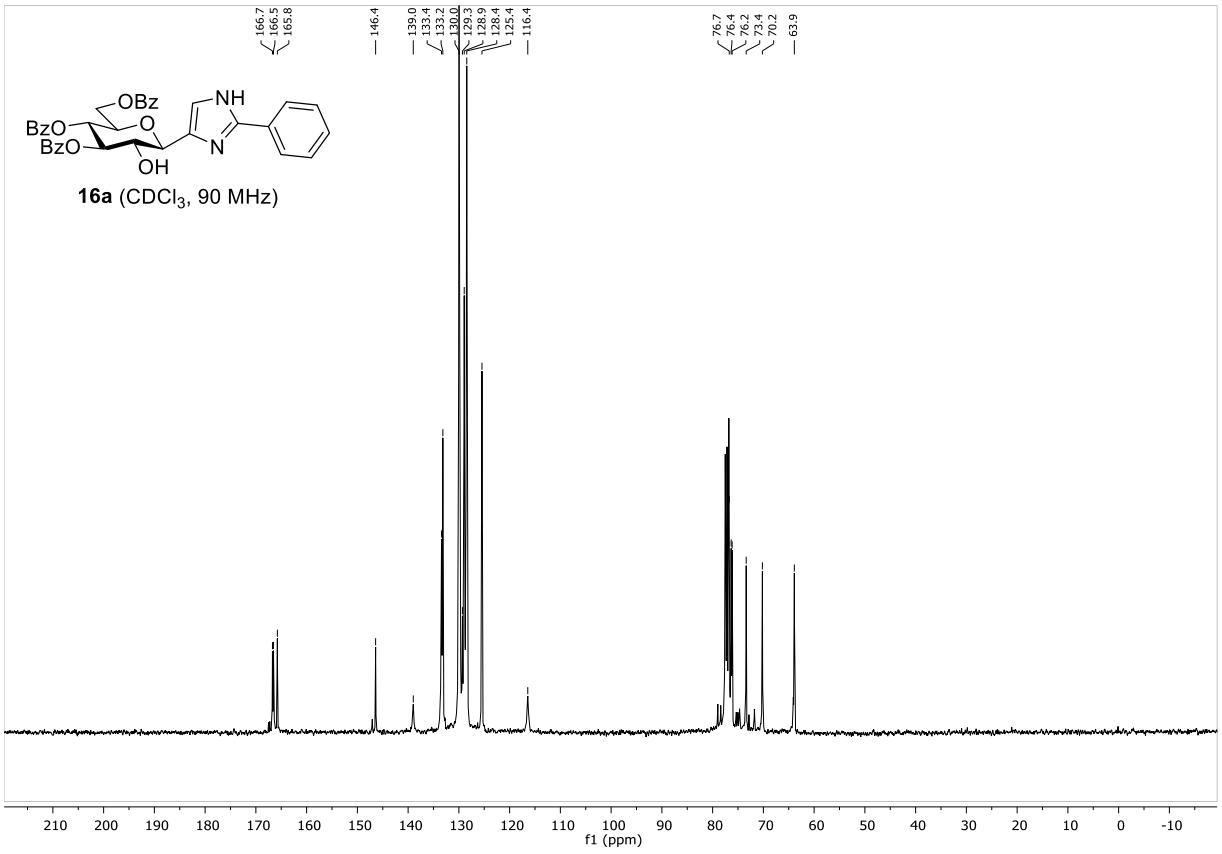
166.7
166.5
165.8
146.4
139.0
133.4
133.2
130.0
129.3
128.9
128.4
125.4
116.4
76.7
76.4
76.2
73.4
70.2
63.9
OBz
NH
BzO
O
BzO
N
OH
16a (CDCl3, 90 MHz)
f1 (ppm)

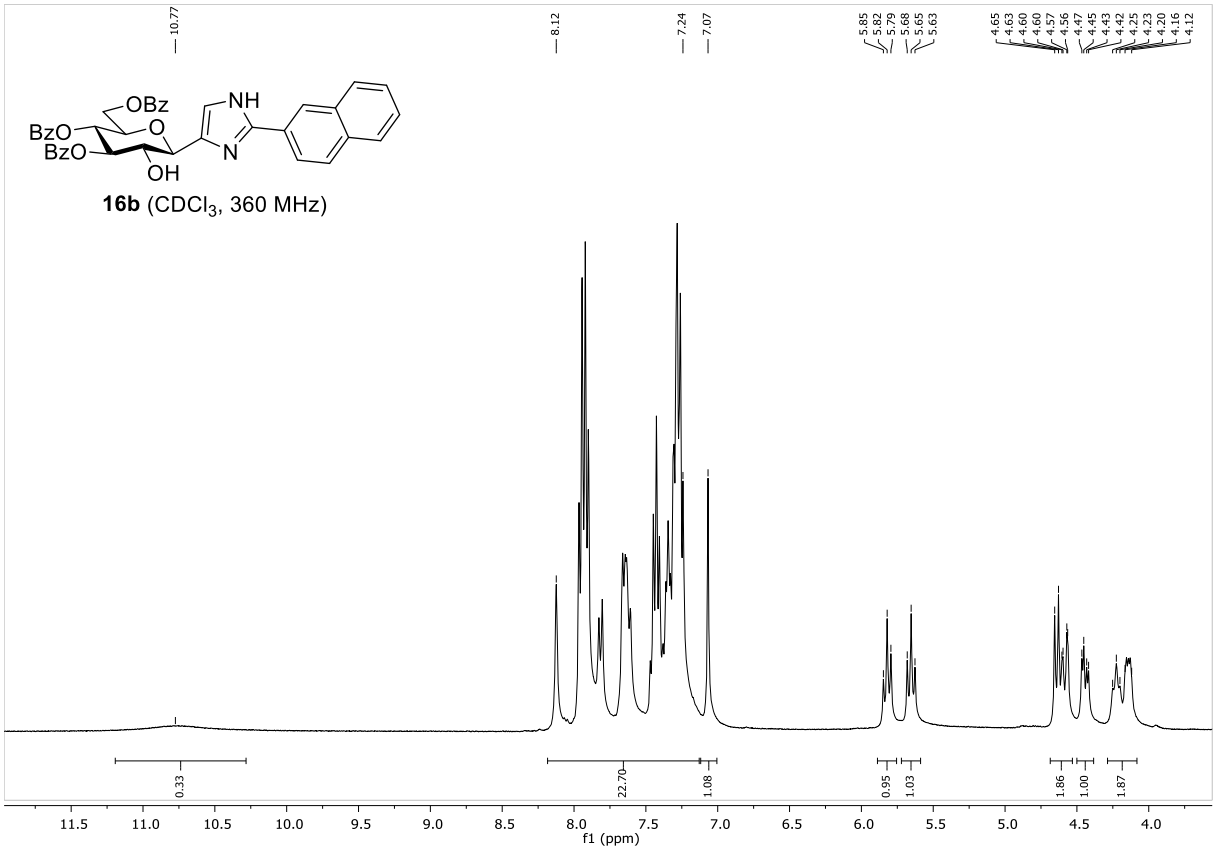
10.77
8.12
7.24
7.07
5.85
5.82
5.79
5.68
5.65
5.63
4.65
4.63
4.60
4.60
4.57
4.56
4.47
4.45
4.43
4.42
4.25
4.23
4.20
4.16
4.12
OBz
NH
BzO
O
BzO
N
OH
16b (CDCl3, 360 MHz)
0.33
22.70
1.08
0.95
1.03
1.86
1.00
1.87
11.5
11.0
10.5
10.0
9.5
9.0
8.5
8.0
7.5
7.0
6.5
6.0
5.5
5.0
4.5
4.0
f1 (ppm)

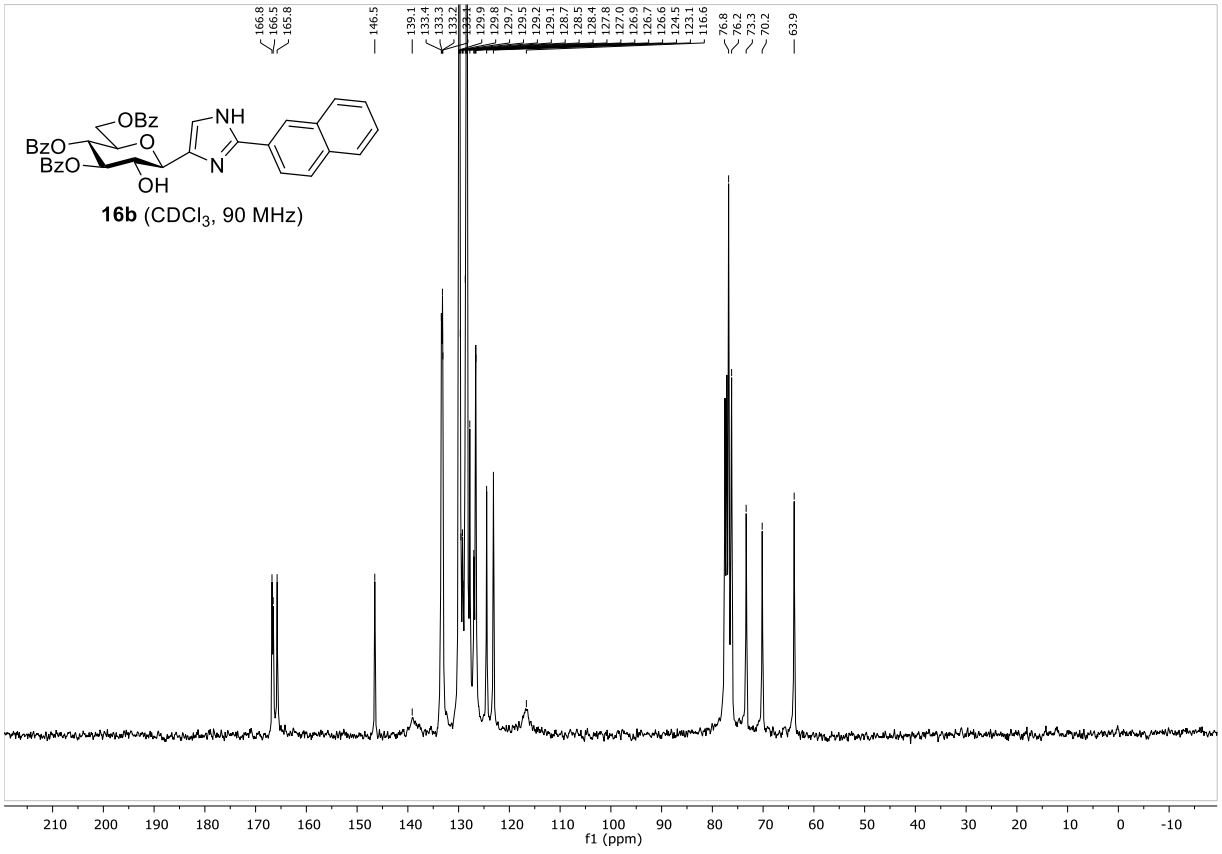
166.8
166.5
165.8
146.5
139.1
133.4
133.3
133.2
129.9
129.8
129.7
129.5
129.2
129.1
128.7
128.5
128.4
127.8
127.0
126.9
126.7
126.6
124.5
123.1
116.6
76.8
76.2
73.3
70.2
63.9
OBz
NH
BzO
O
BzO
N
OH
16b (CDCl3, 90 MHz)
210
200
190
180
170
160
150
140
130
120
110
100
90
80
70
60
50
40
30
20
10
0
-10
f1 (ppm)

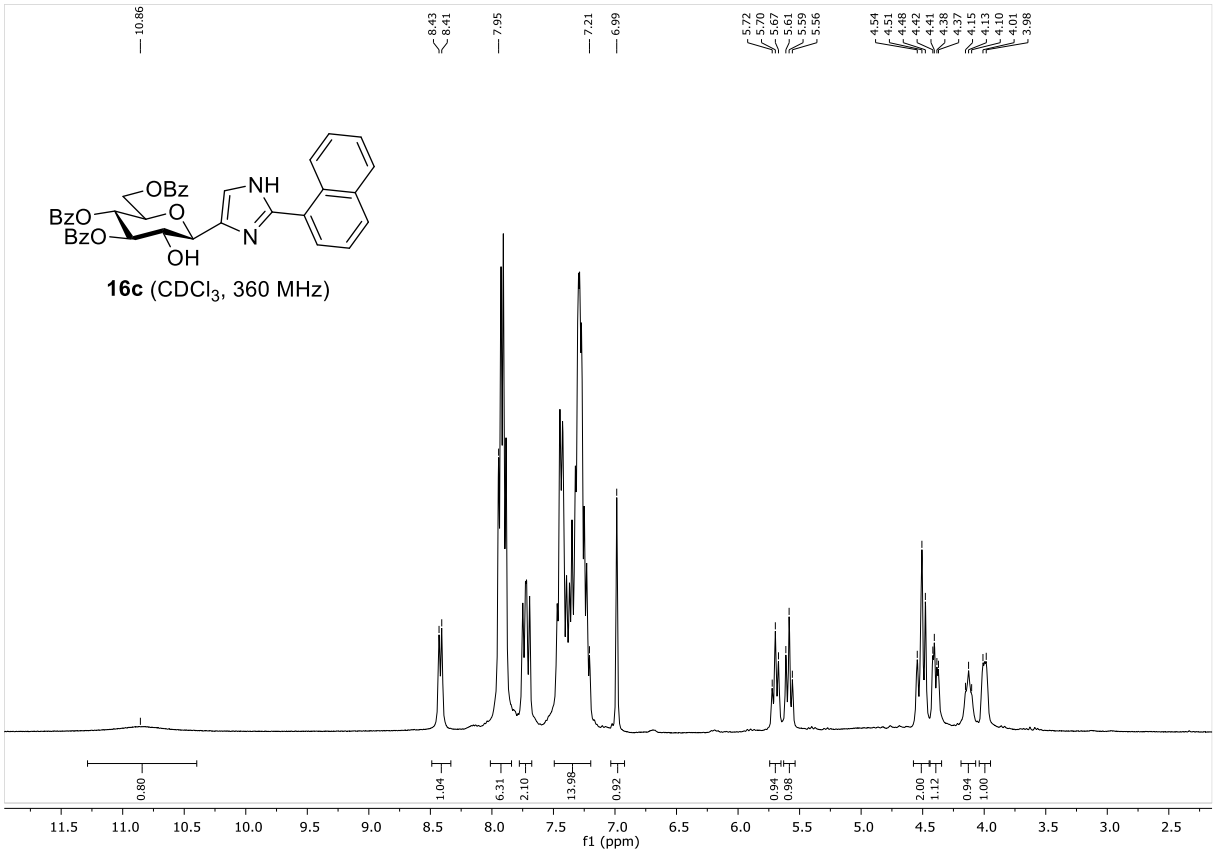
10.86
8.43
8.41
7.95
7.21
6.99
5.72
5.70
5.67
5.61
5.59
5.56
4.54
4.51
4.48
4.42
4.41
4.38
4.37
4.15
4.13
4.10
4.01
3.98
OBz
NH
BzO
O
BzO
N
OH
16c (CDCl3, 360 MHz)
0.80
1.04
6.31
2.10
13.98
0.92
0.94
0.98
2.00
1.12
0.94
1.00
f1 (ppm)

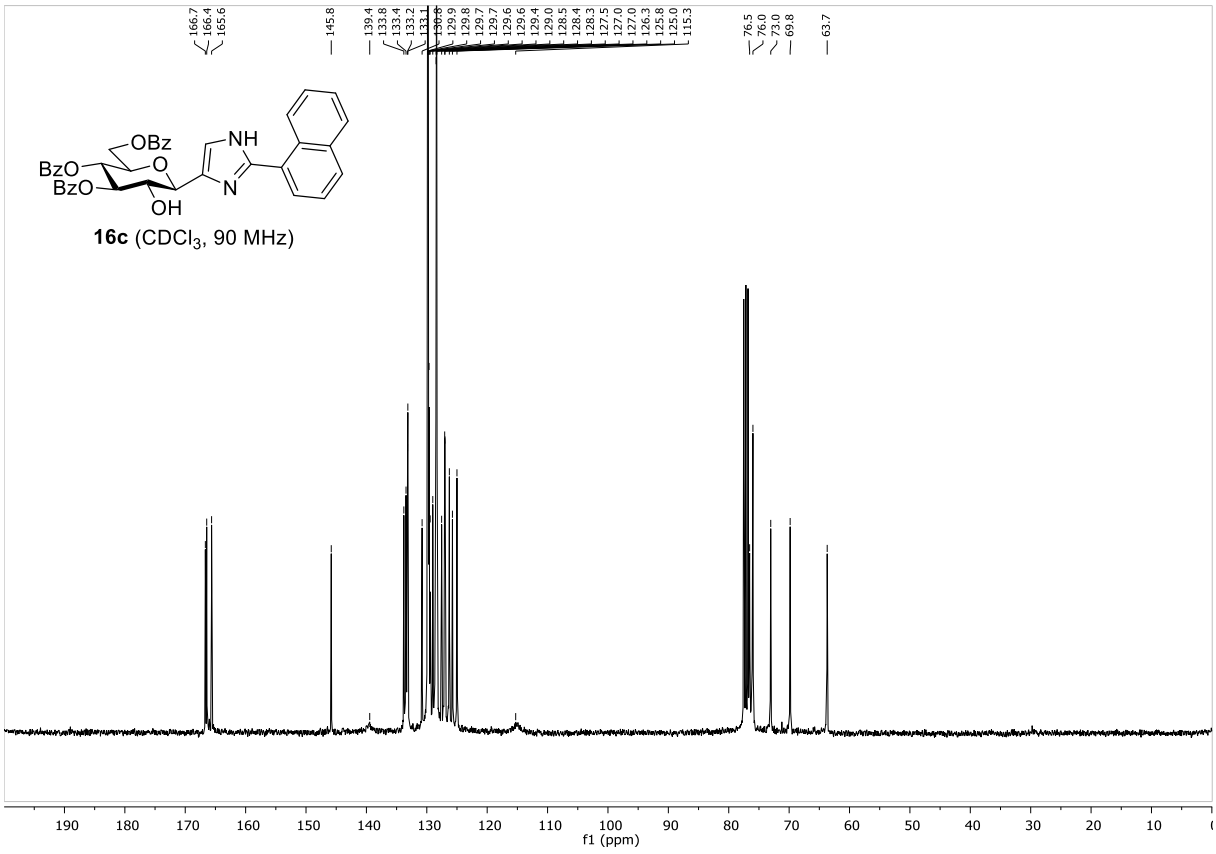
166.7
166.4
165.6
145.8
139.4
133.8
133.4
133.2
133.1
130.8
129.9
129.8
129.7
129.7
129.6
129.6
129.4
129.0
128.5
128.4
128.3
127.5
127.0
127.0
126.3
125.8
125.0
115.3
76.5
76.0
73.0
69.8
63.7
OBz
NH
BzO
O
BzO
N
OH
16c (CDCl3, 90 MHz)
f1 (ppm)

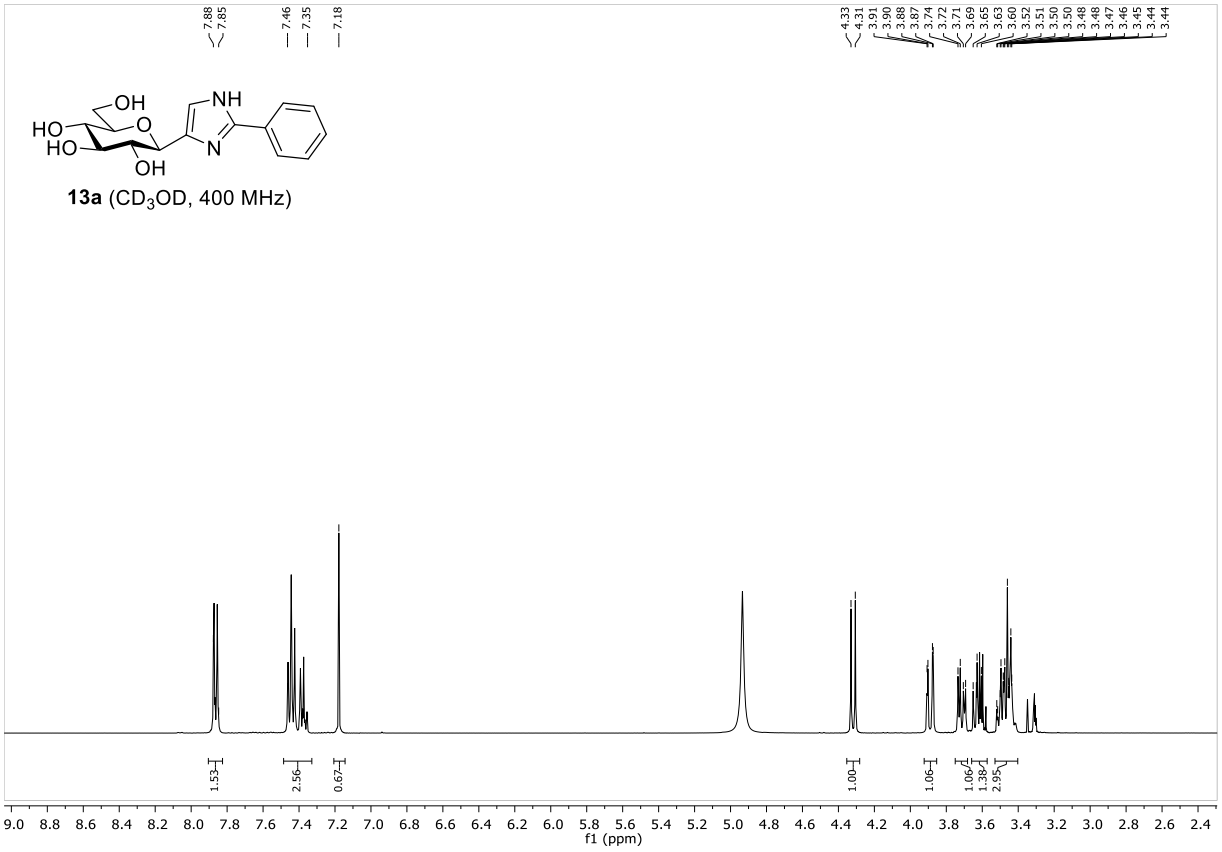

13a (CD_3OD, 400 MHz)

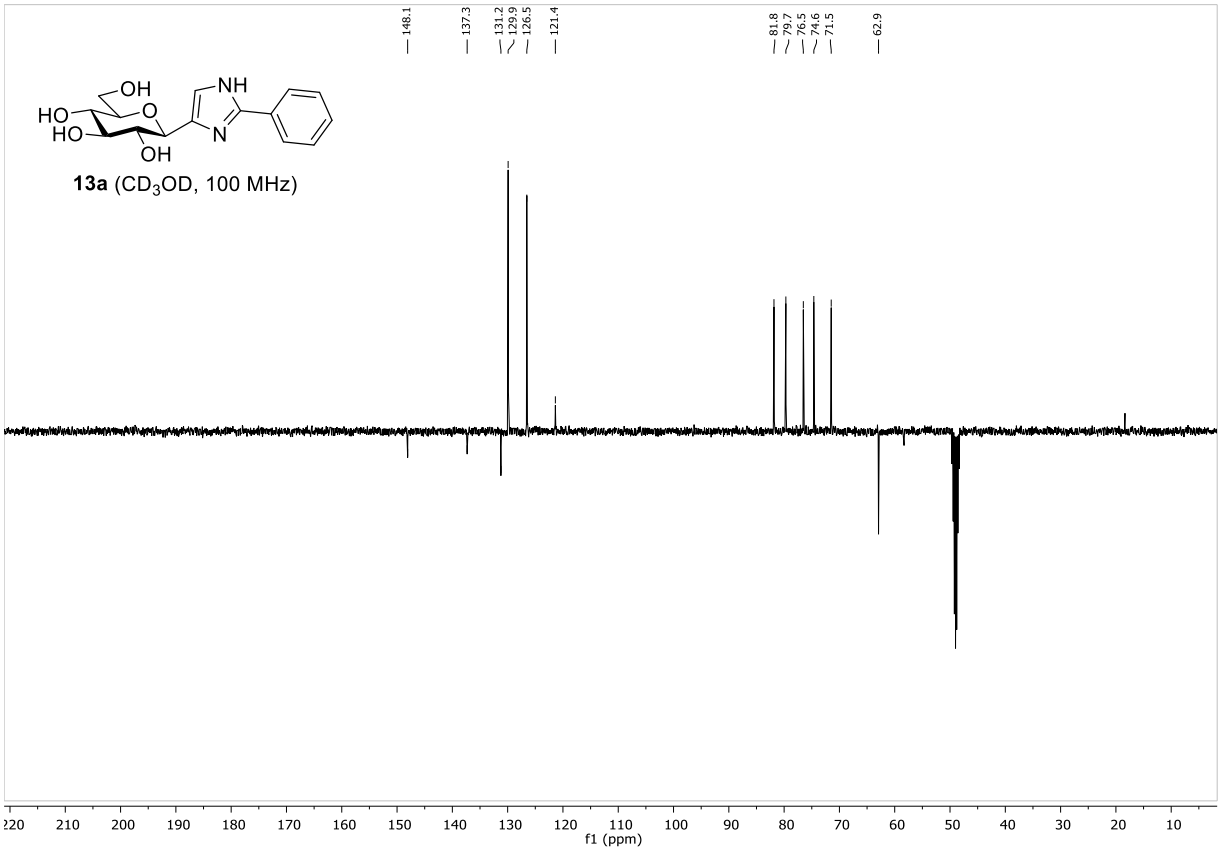

13a (CD_3OD, 100 MHz)

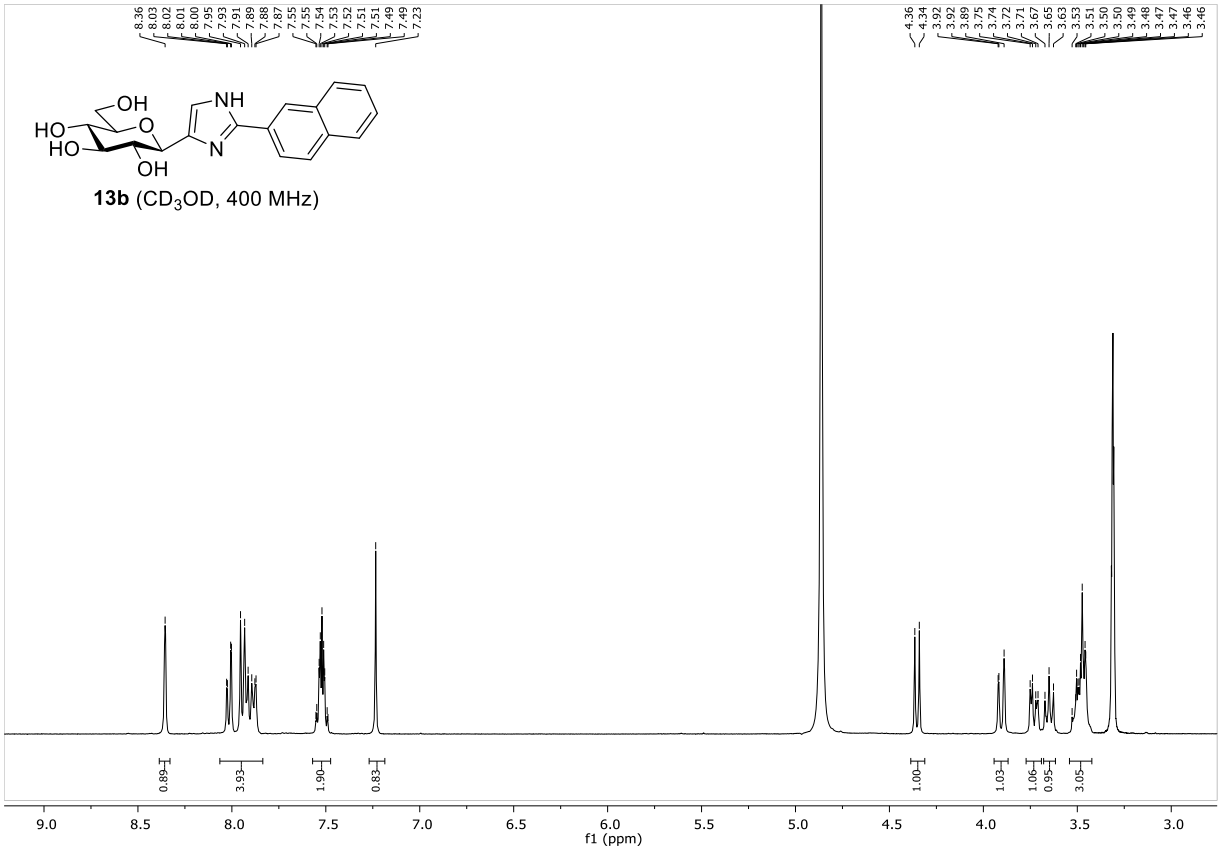

13b (CD_3OD, 400 MHz)

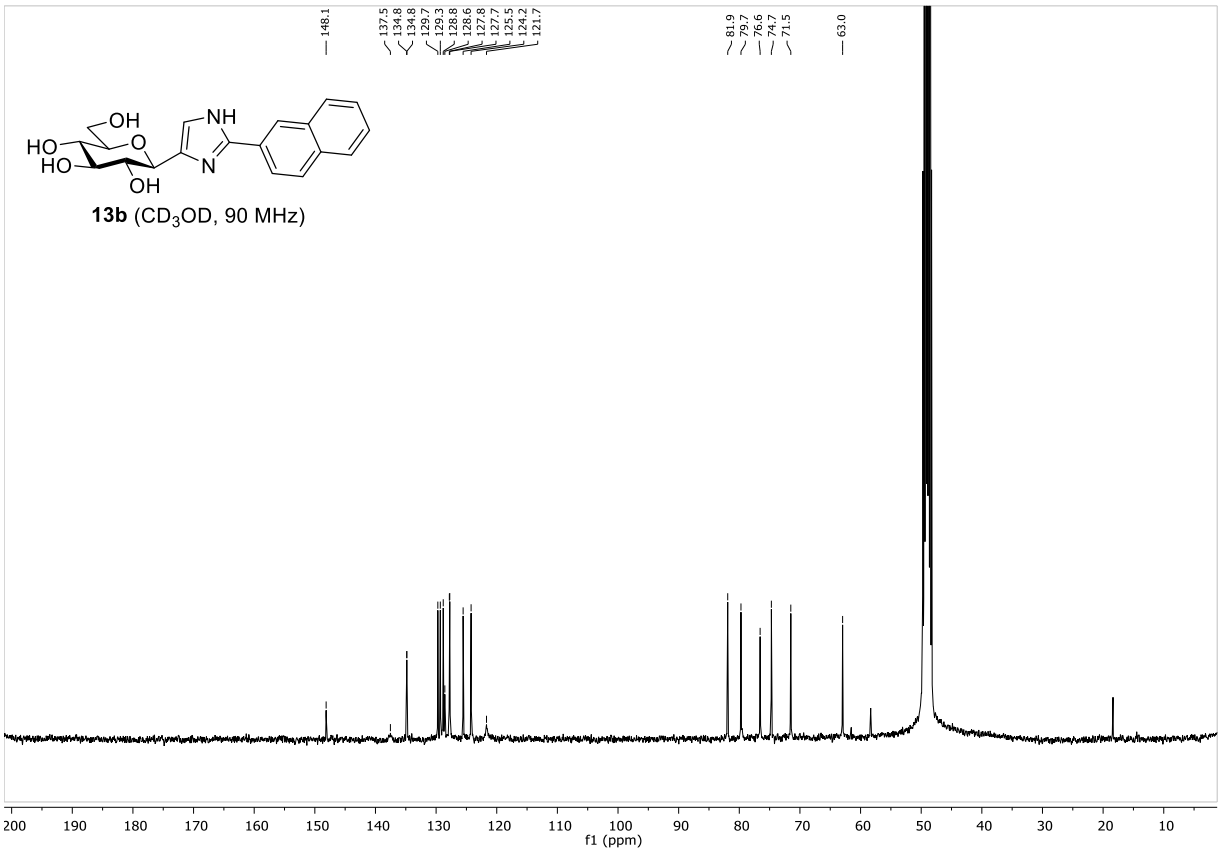

13b (CD_3OD, 90 MHz)

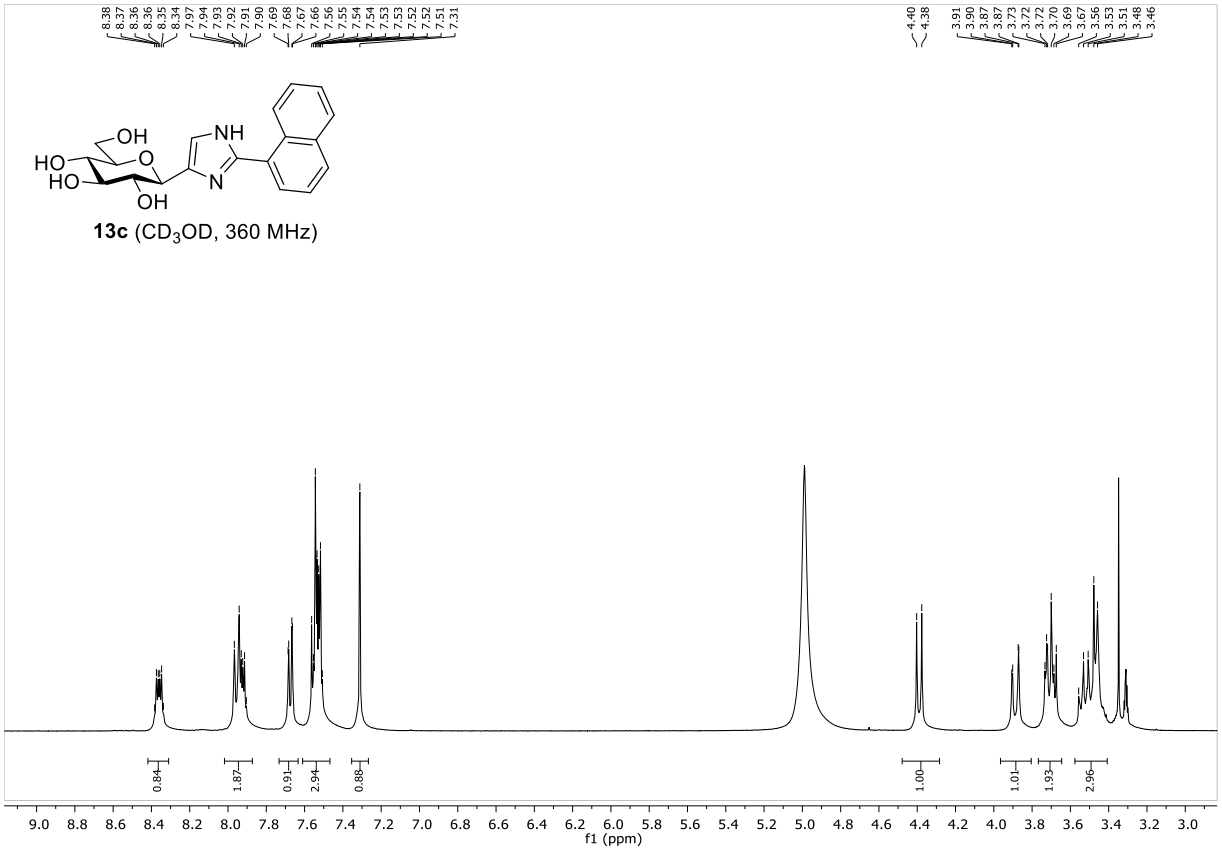
8.38
8.37
8.36
8.36
8.35
8.34
7.97
7.94
7.93
7.92
7.91
7.90
7.69
7.68
7.67
7.66
7.56
7.55
7.54
7.54
7.53
7.53
7.52
7.52
7.51
7.31
4.40
4.38
3.91
3.90
3.87
3.87
3.73
3.72
3.72
3.70
3.69
3.67
3.56
3.53
3.51
3.48
3.46
OH
NH
HO
O
HO
N
OH
13c (CD3OD, 360 MHz)
0.84
1.87
0.91
2.94
0.88
1.00
1.01
1.93
2.96
9.0 8.8 8.6 8.4 8.2 8.0 7.8 7.6 7.4 7.2 7.0 6.8 6.6 6.4 6.2 6.0 5.8 5.6 5.4 5.2 5.0 4.8 4.6 4.4 4.2 4.0 3.8 3.6 3.4 3.2 3.0
f1 (ppm)

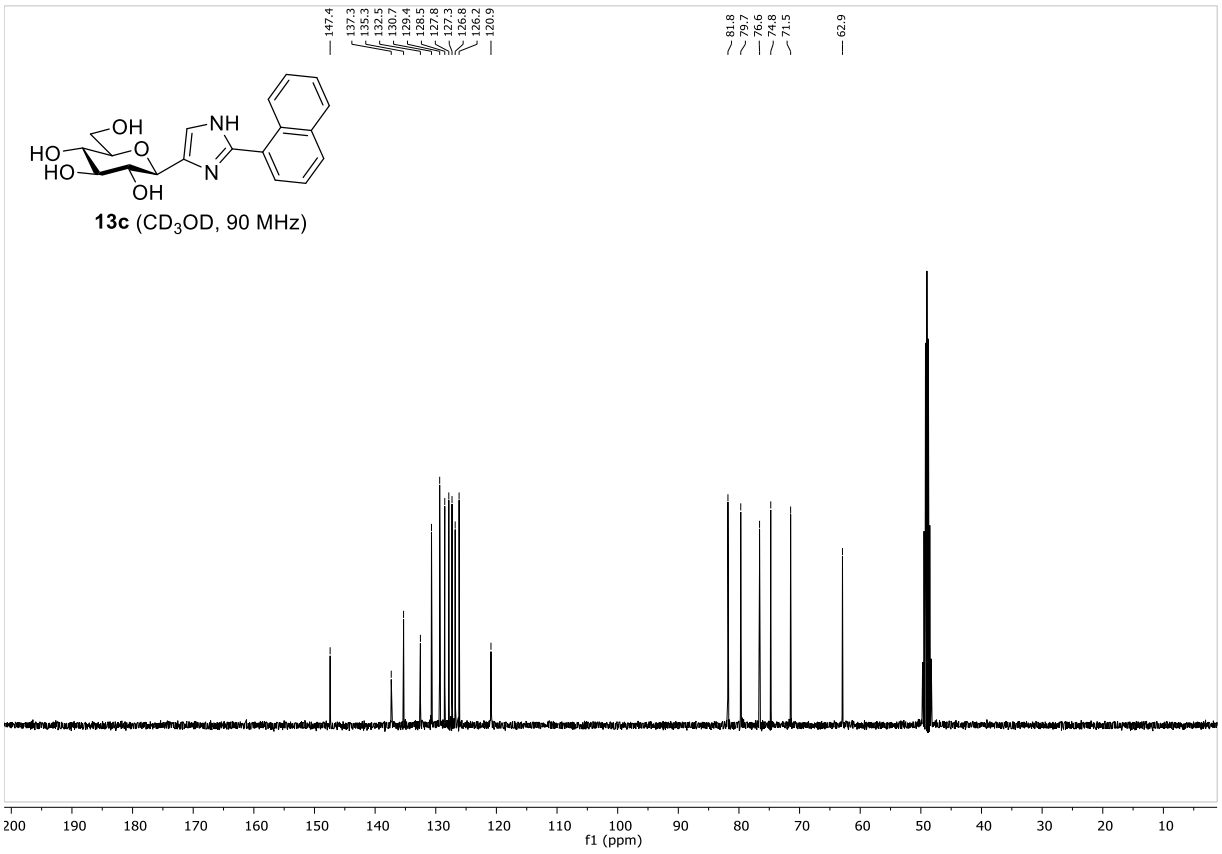
147.4
137.3
135.3
132.5
130.7
129.4
128.5
127.8
127.3
126.8
126.2
120.9
81.8
79.7
76.6
74.8
71.5
62.9
OH
NH
HO
O
HO
N
OH
13c (CD3OD, 90 MHz)
200 190 180 170 160 150 140 130 120 110 100 90 80 70 60 50 40 30 20 10
f1 (ppm)

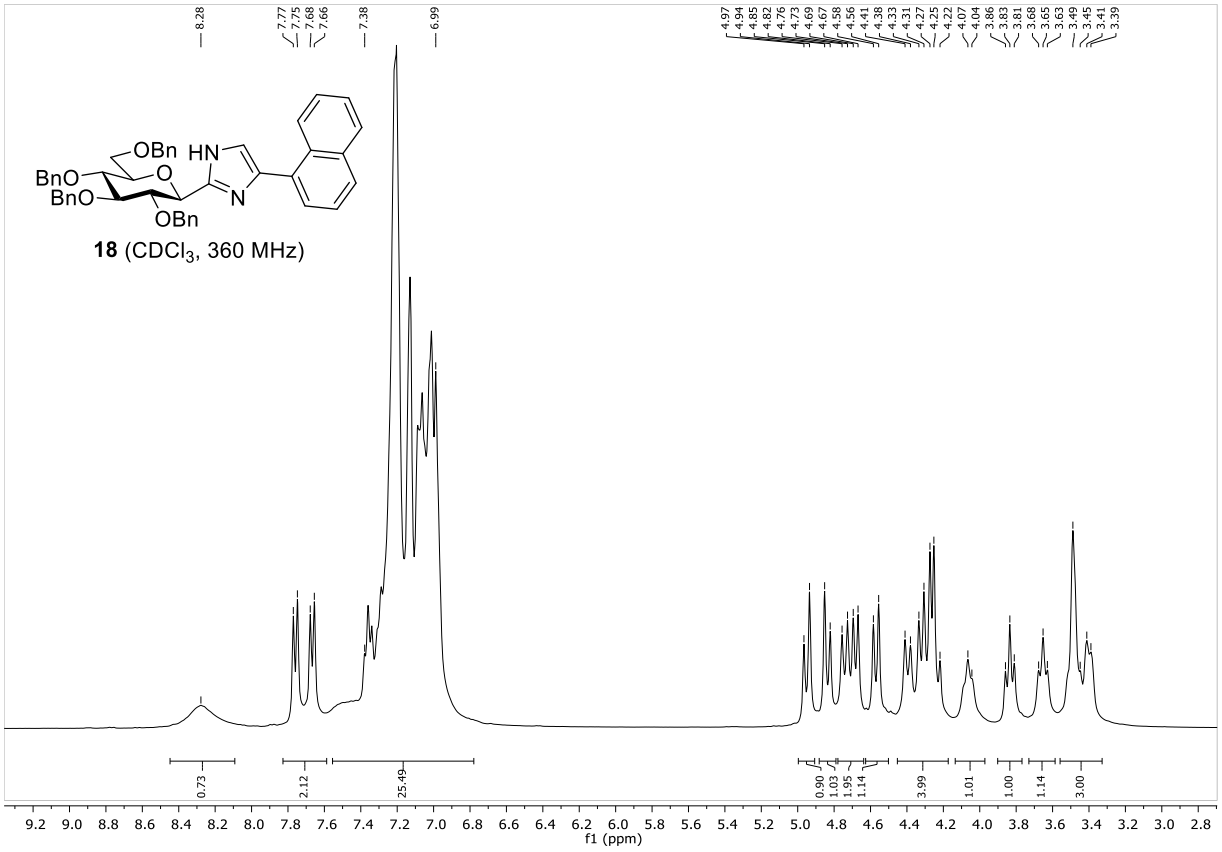

18 ($CDCl_3$, 360 MHz)

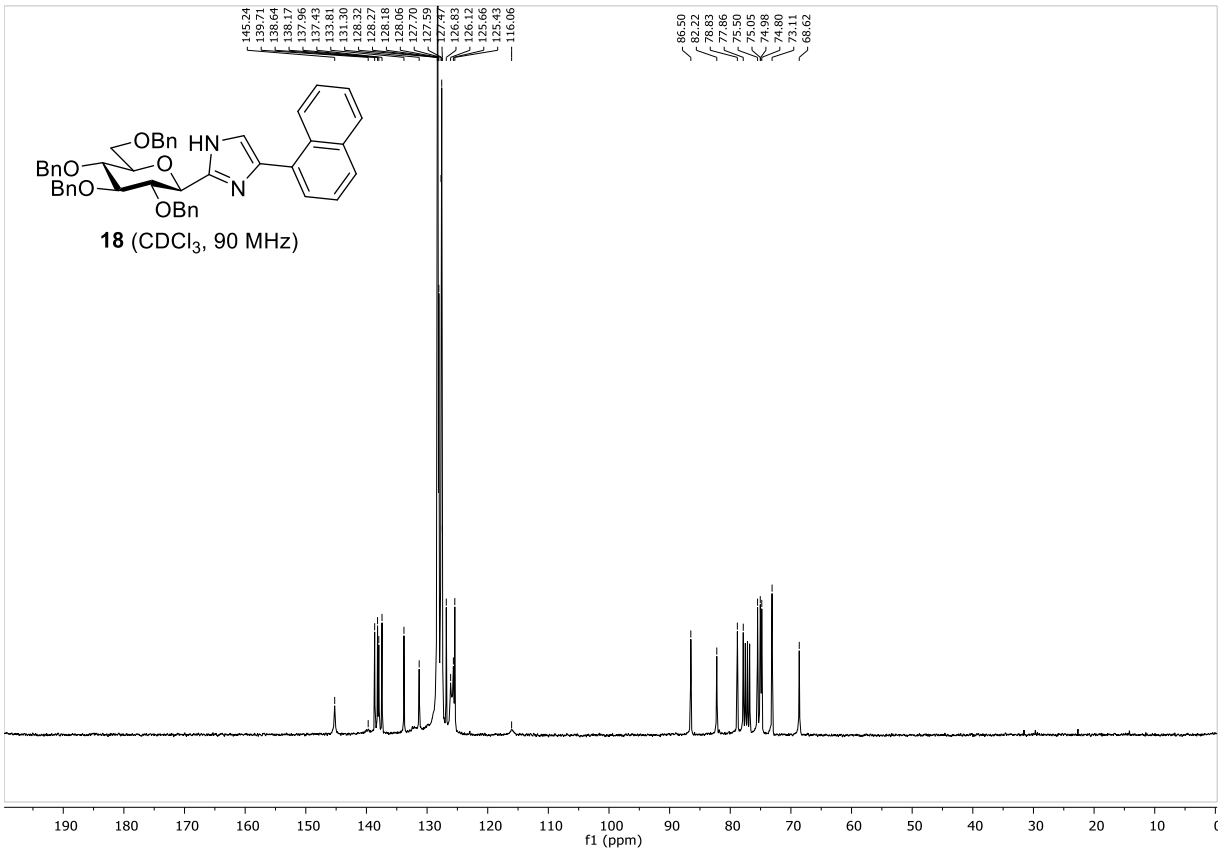

18 ($CDCl_3$, 90 MHz)

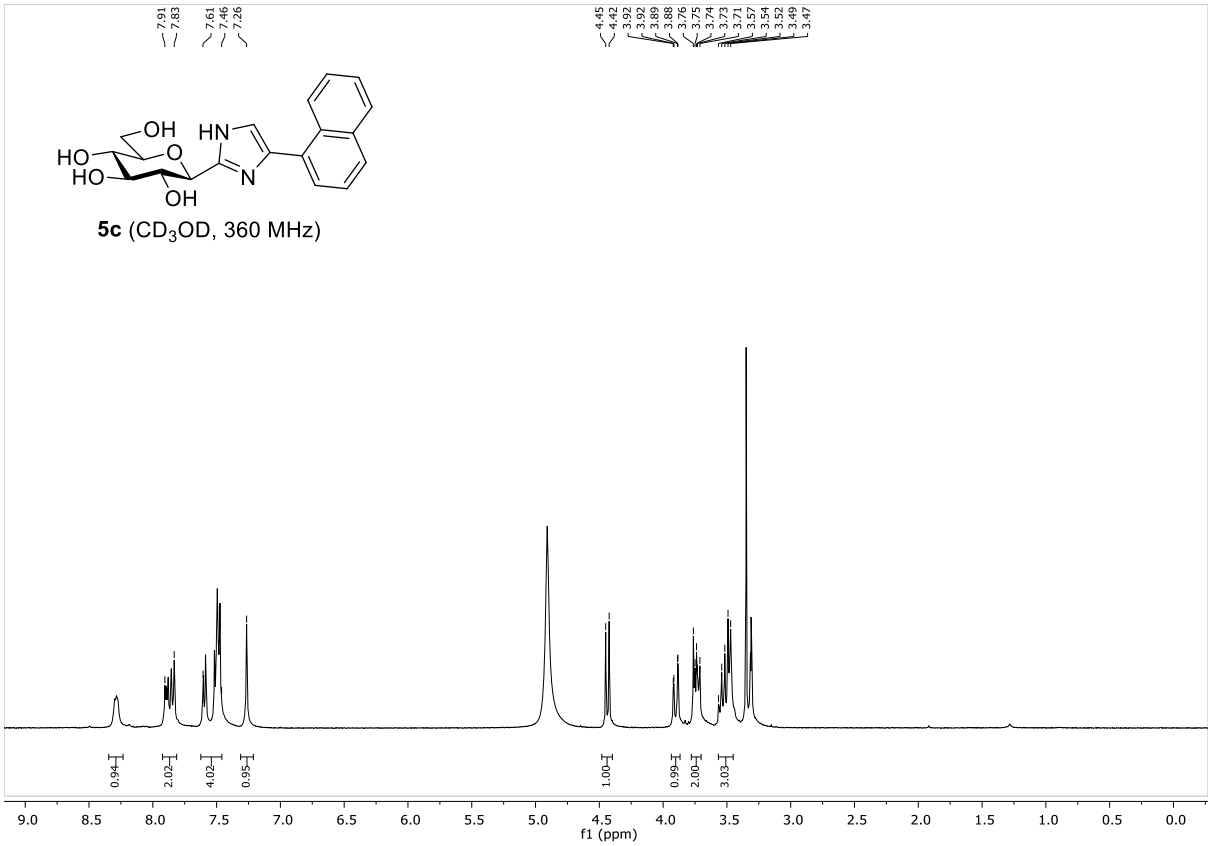

5c (CD_3OD, 360 MHz)

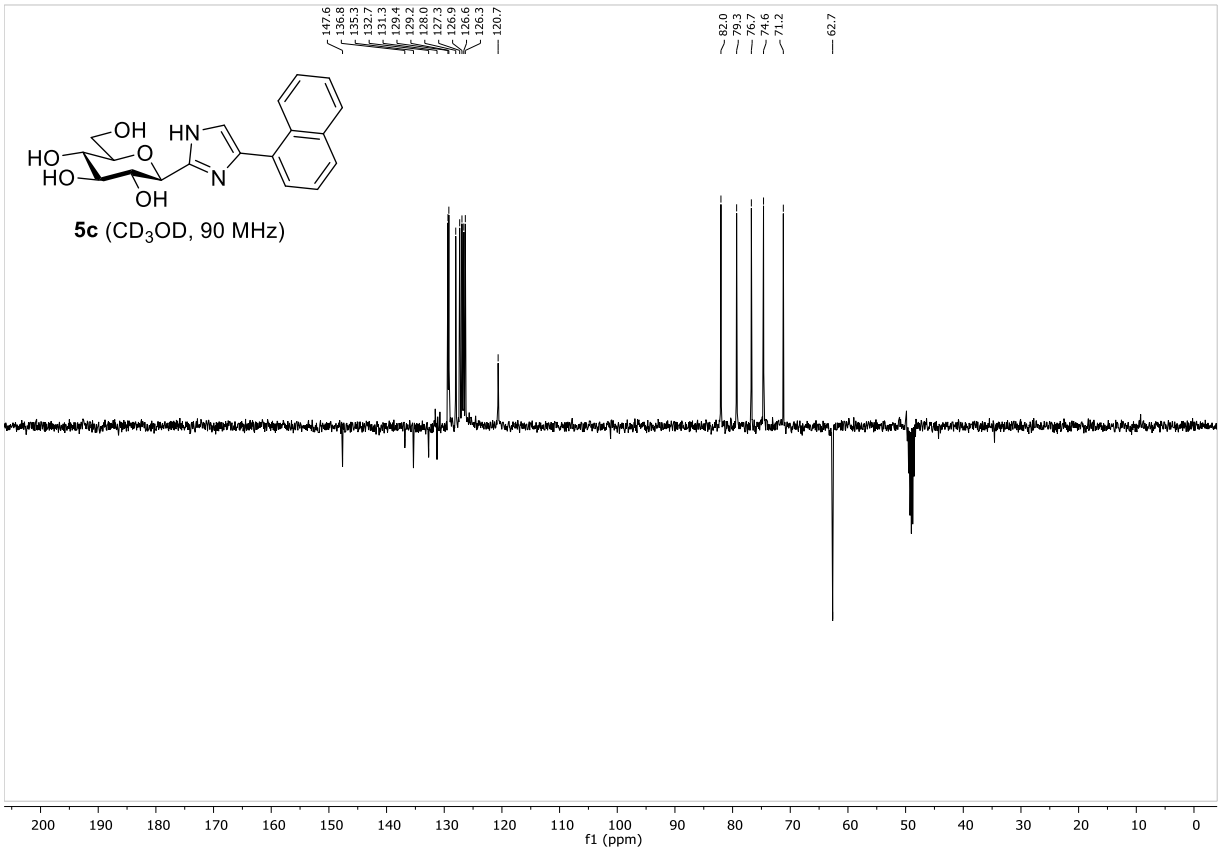

5c (CD_3OD, 90 MHz)

3. Kinetics

Enzyme activity was assayed into the direction of glycogen synthesis at 30°C. Kinetic data were collected using muscle dephosphorylated glycogen phosphorylase *b* (GP*b*) isoform. Kinetic data for the inhibition of GP*b* by glucose analogues were measured in the presence of 10 µg/ml enzyme, various concentrations of α-D-glucose-1-phosphate (4-14 mM) and inhibitors, constant concentration (1%) of glycogen and AMP (1 mM). Enzymatic activities were presented in the form of double-reciprocal plot (Lineweaver-Burk). The plots were analysed by a non-linear data analysis program. The inhibitor constants (K_i) were determined by secondary plots, replotting the slopes from the Lineweaver-Burk plot against the inhibitor concentrations. The means of standard errors for all calculated kinetic parameters averaged to less than 10%.[26-27]

To show the inhibition type, the primary data were subjected to Dixon plot analysis. Concentrations of the inhibitors were as follows:

5c: 2, 3, 4, 5 and 6 µM.

12b: 100, 150, 200, 250 and 300 µM.

13a: 150, 187.5, 225, 262.5 and 300 µM.

13b: 3, 6, 9, 12 and 15 µM.

13c: 150, 200, 250, 300 and 350 µM.

The plots are shown below and the intersection in the negative region of the abscissa indicate competitive inhibition.

5c

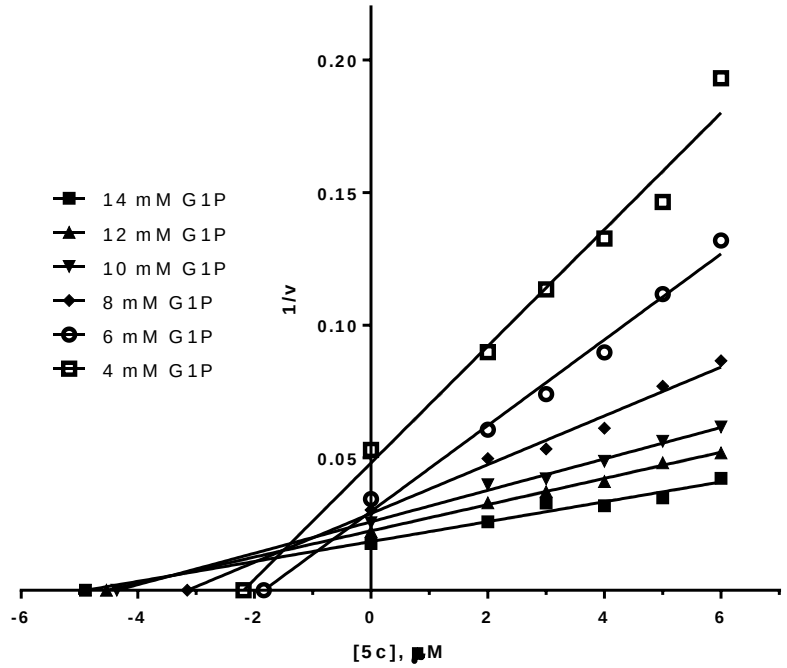
14 mM G1P
12 mM G1P
10 mM G1P
8 mM G1P
6 mM G1P
4 mM G1P
1/v
0.20
0.15
0.10
0.05
-6
-4
-2
0
2
4
6
[5c], μM

12b

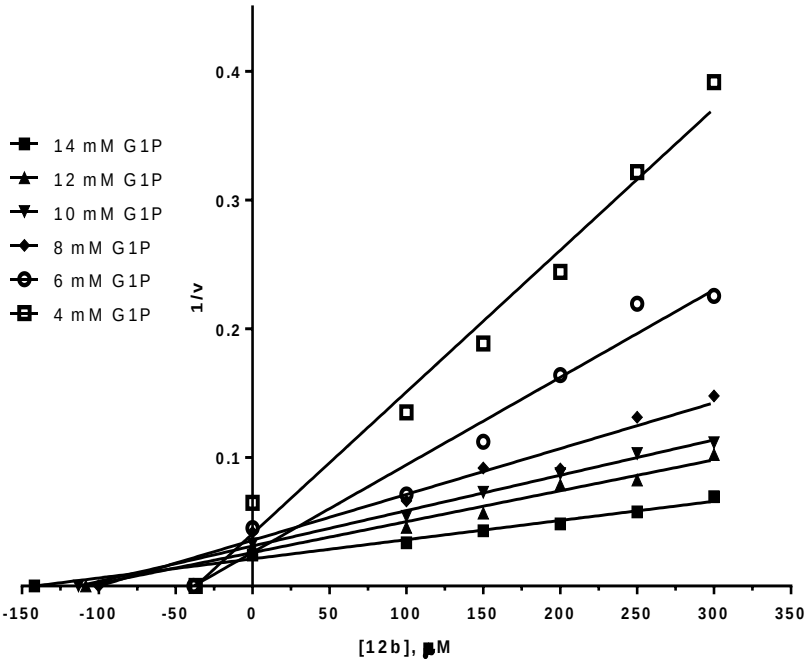
14 mM G1P
12 mM G1P
10 mM G1P
8 mM G1P
6 mM G1P
4 mM G1P
1/v
0.4
0.3
0.2
0.1
-150
-100
-50
0
50
100
150
200
250
300
350
[12b], μM

13a

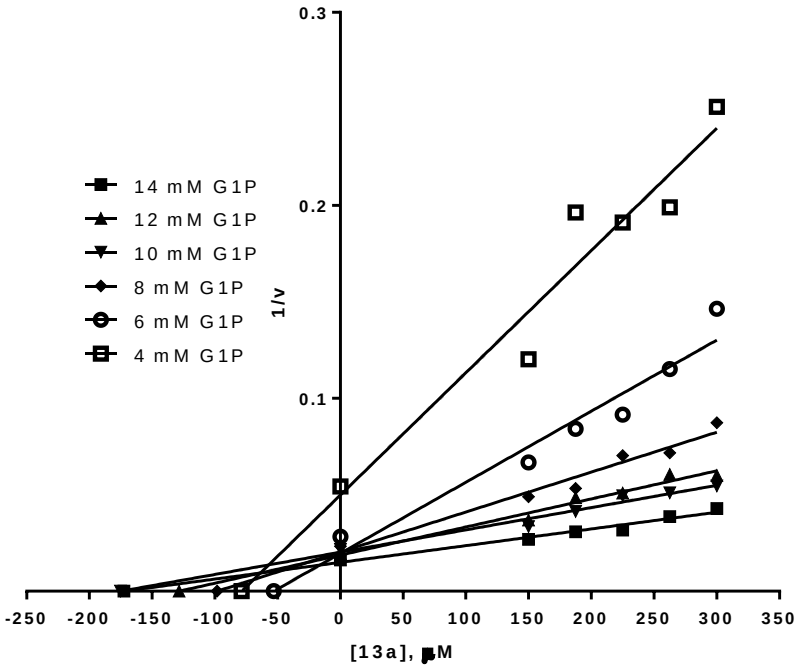
14 mM G1P
12 mM G1P
10 mM G1P
8 mM G1P
6 mM G1P
4 mM G1P
1/v
0.3
0.2
0.1
-250 -200 -150 -100 -50 0 50 100 150 200 250 300 350
[13a], µM

13b

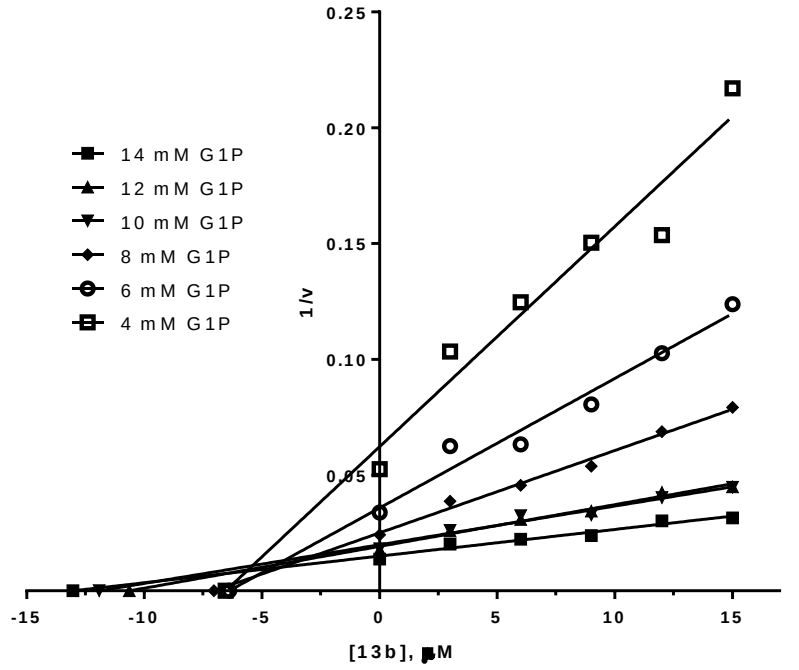
14 mM G1P
12 mM G1P
10 mM G1P
8 mM G1P
6 mM G1P
4 mM G1P
1/v
0.25
0.20
0.15
0.10
0.05
-15 -10 -5 0 5 10 15
[13b], µM

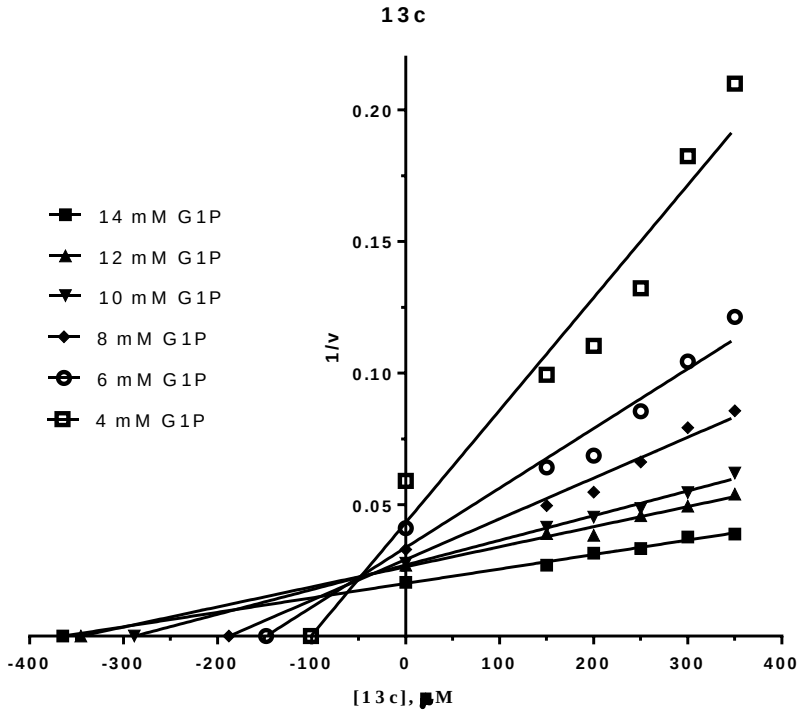

4. *Ex-vivo* Experiments

Hepatocytes were isolated from adult male C57BL/6N mice (aged 8 to 12 weeks). Mice were maintained in individually ventilated cages and environmental conditions as outlined in the Home Office Code of Practice. Procedures conformed to Home Office Regulations and were approved by Newcastle University Ethics Committee. Mice were euthanized with isoflurane overdose and heparin-injected followed by laparotomy and liver perfusion through the inferior vena cava. The liver was perfused at 5 ml/min for 5 min with Ca-free Hanks buffer followed by 15 min with Hanks buffer containing 0.1 mg/ml collagenase (Sigma C5138). The liver was dissociated and the hepatocytes sedimented at 50 g, and then suspended in Minimum Essential Medium (MEM, Life Technologies 21430) supplemented with 5% (v/v) newborn calf serum, 10nM dexamethasone and 10nM insulin and seeded on gelatin-coated (0.1% wt/vol) 12-well plates. After cell attachment (4 h) the medium was replaced by serum-free MEM containing 25 mM glucose, 10 nM dexamethasone, 10 nM insulin and the hepatocytes were cultured

overnight. Incubations for determination of glycogenolysis were performed after 20 h culture in glucose-free DMEM (Life Technologies, A14430) without or with 200 nM glucagon (Sigma, G2044). With the exception of DAB (1,4-dideoxy-1,4-imino-D-arabinitol, Sigma D1542) which was dissolved in water, all other compounds were prepared in DMSO and the final concentration of DMSO was 0.1% (vol/vol). After overnight culture, the medium was aspirated and the monolayers were washed 3 times in glucose-free medium and then incubated for 3h in glucose-free DMEM containing glucagon and the inhibitors or DMSO alone together with additional controls without glucagon. On termination of the incubation the media was collected for analysis of glucose by the hexokinase, glucose 6-phosphate dehydrogenase coupled assay.[28] Results are expressed as percentage glucose release relative to glucagon containing controls and IC_{50} was determined relative to maximum inhibition by the reference compound DAB. Results are means ± SEM for 4 hepatocytes isolations.

5. References

1. *Schrödinger*, LLC: New York, NY, 2018.
2. Kantsadi, A. L.; Bokor, É.; Kun, S.; Stravodimos, G. A.; Chatzileontiadou, D. S.; Leonidas, D. D.; Juhász-Tóth, É.; Szakács, A.; Batta, G.; Docsa, T.; Gergely, P.; Somsák, L., Synthetic, enzyme kinetic, and protein crystallographic studies of *C*-β-D-glucopyranosyl pyrroles and imidazoles reveal and explain low nanomolar inhibition of human liver glycogen phosphorylase. *European Journal of Medicinal Chemistry* **2016,** *123*, 737-745.
3. Sondergaard, C. R.; Olsson, M. H. M.; Rostkowski, M.; Jensen, J. H., Improved Treatment of Ligands and Coupling Effects in Empirical Calculation and Rationalization of pK(a) Values. *Journal of Chemical Theory and Computation* **2011,** *7* (7), 2284-2295.
4. Harder, E.; Damm, W.; Maple, J.; Wu, C. J.; Reboul, M.; Xiang, J. Y.; Wang, L. L.; Lupyan, D.; Dahlgren, M. K.; Knight, J. L.; Kaus, J. W.; Cerutti, D. S.; Krilov, G.; Jorgensen, W. L.; Abel, R.; Friesner, R. A., OPLS3: A Force Field Providing Broad Coverage of Drug-like Small Molecules and Proteins. *Journal of Chemical Theory and Computation* **2016,** *12* (1), 281-296.
5. Zhao, Y.; Truhlar, D. G., The M06 suite of density functionals for main group thermochemistry, thermochemical kinetics, noncovalent interactions, excited states, and transition elements: two new functionals and systematic testing of four M06-class functionals and 12 other functionals. *Theoretical Chemistry Accounts* **2008,** *120* (1-3), 215-241.
6. Hehre, W. J.; Ditchfie.R; Pople, J. A., Self-Consistent Molecular-Orbital Methods .12. Further Extensions of Gaussian-Type Basis Sets for Use in Molecular-Orbital Studies of Organic-Molecules. *Journal of Chemical Physics* **1972,** *56* (5), 2257-2261.

7. Francl, M. M.; Pietro, W. J.; Hehre, W. J.; Binkley, J. S.; Gordon, M. S.; Defrees, D. J.; Pople, J. A., Self-Consistent Molecular-Orbital Methods .23. A Polarization-Type Basis Set for 2nd-Row Elements. *Journal of Chemical Physics* **1982,** *77* (7), 3654-3665.
8. Marenich, A. V.; Olson, R. M.; Kelly, C. P.; Cramer, C. J.; Truhlar, D. G., Self-consistent reaction field model for aqueous and nonaqueous solutions based on accurate polarized partial charges. *Journal of Chemical Theory and Computation* **2007,** *3* (6), 2011-2033.
9. Jones, G.; Willett, P.; Glen, R. C.; Leach, A. R.; Taylor, R., Development and validation of a genetic algorithm for flexible docking. *Journal of Molecular Biology* **1997,** *267* (3), 727-748.
10. Manta, S.; Xipnitou, A.; Kiritsis, C.; Kantsadi, A. L.; Hayes, J. M.; Skamnaki, V. T.; Lamprakis, C.; Kontou, M.; Zoumpoulakis, P.; Zographos, S. E.; Leonidas, D. D.; Komiotis, D., 3 '-Axial CH2OH Substitution on Glucopyranose does not Increase Glycogen Phosphorylase Inhibitory Potency. QM/MM-PBSA Calculations Suggest Why. *Chemical Biology & Drug Design* **2012,** *79* (5), 663-673.
11. Benltifa, M.; Hayes, J. M.; Vidal, S.; Gueyrard, D.; Goekjian, P. G.; Praly, J. P.; Kizilis, G.; Tiraidis, C.; Alexacou, K. M.; Chrysina, E. D.; Zographos, S. E.; Leonidas, D. D.; Archontis, G.; Oikonomakos, N. G., Glucose-based spiro-isoxazolines: A new family of potent glycogen phosphorylase inhibitors. *Bioorganic and Medicinal Chemistry* **2009,** *17* (20), 7368-7380.
12. Tsirkone, V. G.; Tsoukala, E.; Lamprakis, C.; Manta, S.; Hayes, J. M.; Skamnaki, V. T.; Drakou, C.; Zographos, S. E.; Komiotis, D.; Leonidas, D. D., 1-(3-Deoxy-3-fluoro-β-D-glucopyranosyl) pyrimidine derivatives as inhibitors of glycogen phosphorylase b: Kinetic, crystallographic and modelling studies. *Bioorganic and Medicinal Chemistry* **2010,** *18* (10), 3413-3425.
13. Kun, S.; Begum, J.; Kyriakis, E.; Stamati, E. C. V.; Barkas, T. A.; Szennyes, E.; Bokor, É.; Szabó, K. E.; Stravodimos, G. A.; Sipos, Á.; Docsa, T.; Gergely, P.; Moffatt, C.; Patraskaki, M. S.; Kokolaki, M. C.; Gkerdi, A.; Skamnaki, V. T.; Leonidas, D. D.; Somsák, L.; Hayes, J. M., A multidisciplinary study of 3-(β-D-glucopyranosyl)-5-substituted-1,2,4-triazole derivatives as glycogen phosphorylase inhibitors: Computation, synthesis, crystallography and kinetics reveal new potent inhibitors. *European Journal of Medicinal Chemistry* **2018,** *147*, 266-278.
14. Begum, J.; Varga, G.; Docsa, T.; Gergely, P.; Hayes, J. M.; Juhász, L.; Somsák, L., Computationally motivated synthesis and enzyme kinetic evaluation of *N*-(β-D-glucopyranosyl)-1,2,4-triazolecarboxamides as glycogen phosphorylase inhibitors. *Medchemcomm* **2015,** *6* (1), 80-89.
15. Bokor, É.; Kun, S.; Docsa, T.; Gergely, P.; Somsák, L., 4(5)-Aryl-2-*C*-glucopyranosyl-imidazoles as New Nanomolar Glucose Analogue Inhibitors of Glycogen Phosphorylase. *ACS Medicinal Chemistry Letters* **2015,** *6* (12), 1215-1219.
16. Tóth, M.; Kun, S.; Bokor, É.; Benltifa, M.; Tallec, G.; Vidal, S.; Docsa, T.; Gergely, P.; Somsák, L.; Praly, J. P., Synthesis and structure-activity relationships of C-glycosylated oxadiazoles as inhibitors of glycogen phosphorylase. *Bioorganic and Medicinal Chemistry* **2009,** *17* (13), 4773-4785.
17. Kun, S.; Bokor, É.; Varga, G.; Szőcs, B.; Páhi, A.; Czifrák, K.; Tóth, M.; Juhász, L.; Docsa, T.; Gergely, P.; Somsák, L., New synthesis of 3-(β-D-glucopyranosyl)-5-substituted-1,2,4-triazoles, nanomolar inhibitors of glycogen phosphorylase. *European Journal of Medicinal Chemistry* **2014,** *76*, 567-579.
18. Chrysina, E. D.; Bokor, É.; Alexacou, K. M.; Charavgi, M. D.; Oikonomakos, G. N.; Zographos, S. E.; Leonidas, D. D.; Oikonomakos, N. G.; Somsák, L., Amide-1,2,3-triazole

bioisosterism: the glycogen phosphorylase case. *Tetrahedron-Asymmetry* **2009,** *20* (6-8), 733-740.
19. Bokor, É.; Széles, Z.; Docsa, T.; Gergely, P.; Somsák, L., *C*-Glucopyranosyl-1,2,4-triazol-5-ones: synthesis and inhibition of glycogen phosphorylase. *Carbohydrate Research* **2016,** *429*, 128-134.
20. Szennyes, E.; Bokor, É.; Docsa, T.; Sipos, Á.; Somsák, L., Synthesis of *C*-β-D-glucopyranosyl derivatives of some fused azoles. *Carbohydrate Research* **2019**, 472, 33-41.
21. Szennyes, E.; Bokor, É.; Batta, G.; Docsa, T.; Gergely, P.; Somsák, L., Improved preparation of 4(5)-aryl-2-(β-D-glucopyranosyl)-imidazoles, the most efficient glucose analogue inhibitors of glycogen phosphorylase. *RSC Advances* **2016,** *6*, 94787-94794.
22. Szennyes, E.; Bokor, É.; Kiss, A.; Somsák, L.; Pascal, Y., Preparation of 2,6-anhydro-3,4,5,7-tetra-*O*-benzyl-D-glycero-D-gulo-heptonimidamide. In *Carbohydrate Chemistry: Proven Synthetic Methods*, Vogel, C.; Murphy, P. V., Eds. CRC Press: Boca Raton, 2017; Vol. 4, pp 323-332.
23. Sudheendran, K.; Schmidt, D.; Frey, W.; Conrad, J.; Beifuss, U., Facile synthesis of 3,5-diaryl-1,2,4-triazoles via copper-catalyzed domino nucleophilic substitution/oxidative cyclization using amidines or imidates as substrates. *Tetrahedron* **2014,** *70* (8), 1635-1645.
24. Kaboudin, B.; Elhamifar, D., Phosphorus pentasulfide: A mild and versatile reagent for the preparation of thioamides from nitriles. *Synthesis-Stuttgart* **2006,** (2), 224-226.
25. Lauwagie, S.; Millet, R.; Pommery, J.; Depreux, P.; Henichart, J. P., Expeditious synthesis of 2-aryl substituted imidazolines and imidazoles. *Heterocycles* **2006,** *68* (6), 1149-1162.
26. Ősz, E.; Somsák, L.; Szilágyi, L.; Kovács, L.; Docsa, T.; Tóth, B.; Gergely, P., Efficient inhibition of muscle and liver glycogen phosphorylases by a new glucopyranosylidene-spiro-thiohydantoin. *Bioorganic and Medicinal Chemistry Letters* **1999,** *9* (10), 1385-1390.
27. Oikonomakos, N. G.; Skamnaki, V. T.; Ősz, E.; Szilágyi, L.; Somsák, L.; Docsa, T.; Tóth, B.; Gergely, P., Kinetic and crystallographic studies of glucopyranosylidene spirothiohydantoin binding to glycogen phosphorylase B. *Bioorganic and Medicinal Chemistry* **2002,** *10* (2), 261-268.
28. Stappenbeck, R.; Hodson, A. W.; Skillen, A. W.; Agius, L.; Alberti, K. G. M. M., Optimized Methods to Measure Acetoacetate, 3-Hydroxybutyrate, Glycerol, Alanine, Pyruvate, Lactate and Glucose in Human Blood Using a Centrifugal Analyzer with a Fluorometric Attachment. *Journal of Automatic Chemistry* **1990,** *12* (5), 213-220.